From the Oceans to the Farms

Science and Societal Impacts of Natural Decadal Climate Variability

A report on CRCES's research accomplishments from 2002 to 2017

The Pacific Decadal Oscillation (PDO) Index

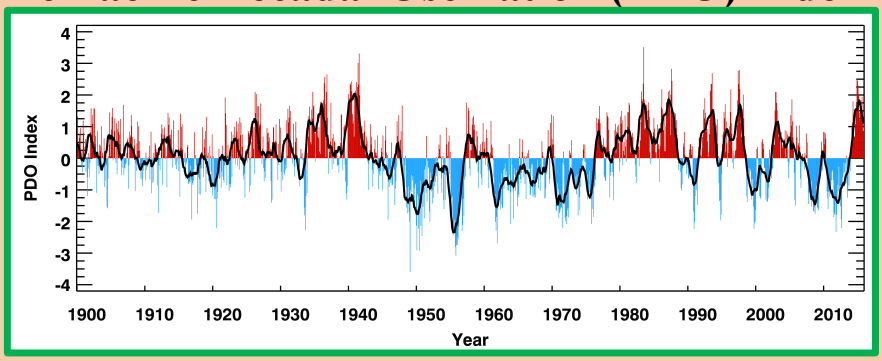

River flow (m^3/s) anomalies in positive and negative PDO years

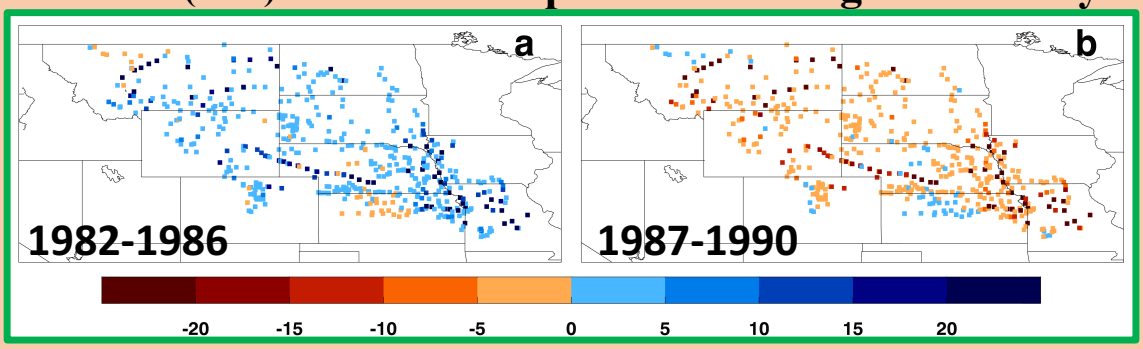

Wheat yield (t/ha) anomalies in positive and negative PDO years

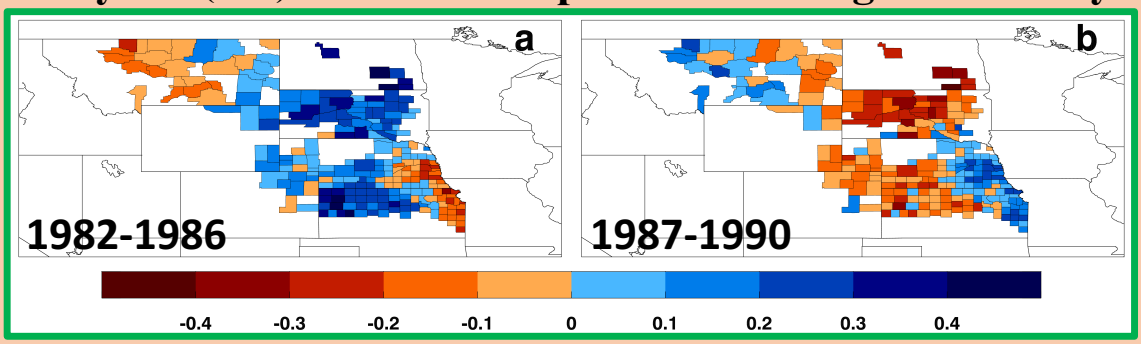

The Center for Research on the Changing Earth System
5523 Research Park Drive, Suite 205, Catonsville, Maryland 21228
missouri.crces.org; mississippi.crces.org; www.crces.org
Phone: 443-543-5493; email: info@crces.org

Contents

Front cover:
Top row: Monthly Pacific Decadal Oscillation (PDO) index.
Middle row: USGS-measured river flow anomalies in the Missouri River Basin (MRB) in positive and negative PDO years.
Bottom row: USDA-NASS estimated, county-aggregated winter wheat yield anomalies in the MRB in positive and negative PDO years.

Foreword

The Center for Research on the Changing Earth System (CRCES) was founded in late 2001 in Maryland as a non-profit, tax-exempt (Internal Revenue Service Code Section 501(c)(3)), scientific research organization. It formally opened an office in July 2002 in Columbia, Maryland. CRCES is governed by a Board of Directors consisting of Dr. Vikram M. Mehta (CRCES), Dr. Norman J. Rosenberg (CRCES), Dr. James J. O'Brien (Florida State University), and Dr. Amita V. Mehta (NASA-UMBC Joint Center for Earth System Technology); Ms. Chetana Neerchal (World Bank) also served as one of the Directors in the initial years. Unfortunately, Dr. O'Brien passed away in the last year and so CRCES lost the guidance he provided.

Although the field of natural decadal climate variability (DCV) and its predictability is at least two centuries old, the field entered a new era in the 1990s due to a gradual release of archives of ocean temperature and salinity data by the world's navies, a gradual understanding of the role of ocean-atmosphere interactions in climate variability, and the development of climate models whose simulations of global climate began to resemble the observed climate. At about the same time, the interannual El Niño-Southern Oscillation's impacts on societal sectors such as water, food, and public health became increasingly evident, with hints of longer term impacts due to natural DCV and potential climate change. These developments instigated CRCES's founding.

In its first decade and a half, CRCES has developed an end-to-end research program from DCV science; to DCV impacts on water, agriculture, and other societal sectors; to extensive and intensive stakeholder interactions. Specific focus areas are:

- DCV, its physics, and its predictability, including possible roles of atmospheric and riverine freshwater fluxes and volcanic eruptions in ocean-atmosphere dynamics and predictability;
- assessments, modeling, and experimental prediction of DCV impacts on water and agriculture, especially in the Missouri River Basin (MRB), a major "bread basket" of not only the U.S. but also the world, and the development of adaptation options;
- assessment and experimental prediction of DCV impacts on the Mississippi River - a major transportation artery for food and other water-borne commerce;
- assessments of decadal climate and societal impacts information needs of stakeholders and policymakers;
- assessment of worldwide impacts of DCV on water including droughts, river flows, agriculture, fisheries, hydro-electricity generation, inland water-borne transportation, and agricultural irrigation; and
- contributions to the evolution of DCV and societal impacts communities.

This report summarizes CRCES's contributions in these areas in the first 15 years.

CRCES's founding and much of its subsequent progress would not have been possible without the encouragement and support provided by Dr. Eric Lindstrom, the Physical Oceanography Program at NASA Headquarters; Dr. Nancy Beller-Simms, the Sectoral Applications Research Program, NOAA-Climate Program Office; and Drs. Nancy Cavallaro and Louie Tupas, the National Institute for Food and Agriculture, U.S. Department of Agriculture. In CRCES's formative years, Dr. Jay Fein, National Science Foundation; and Dr. Anjuli Bamzai, U.S. Department of Energy and National Science Foundation, also provided invaluable advice.

CRCES's progress has been made possible by its people. CRCES has benefitted from Drs. O'Brien and Rosenberg's guidance, and from Dr. A. Mehta's professional expertise and personal support. The research would not have been possible without Drs. Rosenberg, Boyin Huang, and Hui Wang; Ms. Katherin Mendoza; and others. Ms. Janet Wood and Mr. David Wolff initially established and maintained administrative and information technology systems, respectively; these responsibilities were later taken over by Ms. Ann Marie Dubois and Mr. Joseph Jackson, respectively. Ms. Kathy Kahler (Kahler & Associates) and Mr. Chris Scholtes (C.E.A. Scholtes & Associates) have been responsible for accounting and auditing functions. I sincerely thank all the people who have helped CRCES, worked for it, or associated with it in some capacity. They have made CRCES successful in its first decade and a half.

Vikram M. Mehta
Executive Director

1. What is Natural Decadal Climate Variability?

This brief explanation of natural decadal climate variability (DCV) starts with attempts to associate solar variability, as represented by sunspot number variability, with climate variability. Following Schwabe's discovery of the nearly-cyclic variation in sunspot numbers, Wolf found an average cycle length of 11.1 years in historical sunspot observations. In the time series of annual-average Wolf sunspot numbers, the 11-year (or, Schwabe) cycle is prominent and longer term variations are also evident. Sunspot groups with the same magnetic field polarity appear at high solar latitudes at approximately every 22 years or two Schwabe cycles. The 22-year cycle is known as the double sunspot cycle or the Hale cycle. Attempts to relate the 11- and 22-year sunspot variability to climate variability and its societal impacts began well before systematic observations of sunspots began in 1843. It is in these two cyclic periods of sunspot number variability and the attempts to associate climate variability with them that the origin of the phrase "decadal climate variability" or DCV lies. Sir William Herschel hypothesized in 1801 that variations in sunspot numbers implied variations in solar irradiance which might cause variations in atmospheric heating, rainfall, temperature, and agricultural production, and thereby influence the price of wheat in London. Herschel's initial and controversial investigation, motivated by the desire for prediction of agricultural productions and prices, was followed by innumerable subsequent investigations till the early 21st century. Thus, the field of DCV, its impacts, and their prediction is over two centuries old.

The foregoing state of the DCV and impacts research was based on the belief that any climate variations must be forced externally. This paradigm started to shift with the Bjerkenes hypothesis in the 1960s that interactive coupling between atmospheric and oceanic dynamics may be able to generate climate variations even in the absence of variations in external forcing. It was – and still is – generally believed that the atmosphere cannot generate variability at time scales longer than one or two years, at the most, due to its relatively low thermal and mechanical inertia, whereas the much larger inertias of the ocean and its slow to very slow circulations may be able to generate interannual to multidecadal and longer timescale variability on their own. Herein lies the importance of SSTs as an indicator as well as a driver of interannual to multidecadal climate variability. While it is possible that non-linear atmospheric dynamics, especially in winter, may be able to generate interannual to multidecadal and longer timescale variability on its own, the working paradigm since the Bjerkenes hypothesis emphasizes the oceans as the main driver of interannual to multidecadal and longer timescale climate variability.

The end of the Cold War in the early 1990s enabled the public release of long term ocean temperature and salinity data that the U.S., British, Soviet, and other navies held in their archives. These and other data collected by merchant ships since the 1850s soon became available to researchers for analyses. Several poorly quantified or hitherto unknown phenomena emerged from these analyses such as decadal variability of the tropical Atlantic SST gradient (TAG for brevity), the Pacific Decadal Oscillation (PDO)/the Interdecadal Pacific Oscillation, and decadal variability of frequency and intensity of the EN – LN phenomenon. Then, analyses of archived data and their assimilation in models of the atmosphere and the oceans made possible discoveries of decadal–multidecadal variability in long known atmospheric phenomena such as the North Pacific Oscillation, the North Atlantic Oscillation, and the Southern Oscillation; and in the Tropical Warm Pools, adding further richness to the spectrum of natural DCV phenomena. The SST-based efforts to understand and predict decadal hydro-meteorological variations are different from the Sunspot-based efforts to the extent that the hypothesis about how decadal SST variability may be influencing hydro-meteorology on continents is better supported by understanding based on observational and modeling evidence.

Further information about these DCV phenomena are available in Mehta (2017*; Natural Decadal Climate Variability: Societal Impacts.* CRC Press, Boca Raton, 326 pages) and from missouri.crces.org/research/decadal-climate-variability.

2. Research on Natural Decadal Climate Variability and Predictability

2.1 Decadal variability of the Tropical Warm Pools and Its Association with Global Atmospheric Variability

Some of the most important permanent features of the Earth's oceans are the Tropical Warm Pools (TWPs), especially the Indo-Pacific Warm Pool (IPWP) and the west Atlantic Warm Pool (WAWP). The TWPs contain much of the warmest and freshest surface ocean water on the Earth. Annual-average sea-surface temperatures (SSTs) in the TWP regions usually exceed 28°C (Fig. 1).

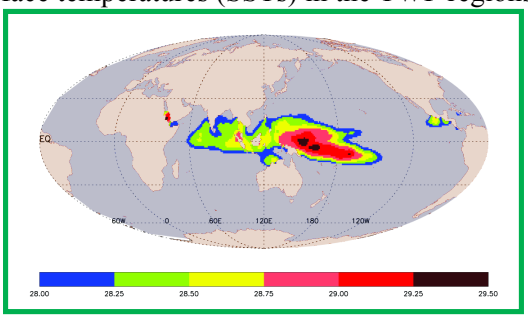

Figure 1: The Indo-Pacific Warm Pool as outlined by SSTs ≥ 28°C.

Since saturation vapor pressure is an exponential function of SST, there can be a dramatic increase in atmospheric convection over the TWPs when the SST exceeds a threshold, typically 28°C-28.5°C. Therefore, even small changes in the TWP SST can cause large changes in atmospheric convection locally. Such a change can significantly modify atmospheric boundary layer and convective processes locally, and substantially impact global atmospheric heating and planetary-scale wave activity. The annual, long-term average area of the IPWP on the eastern Indian Ocean side is approximately 6 million sq. km and on the western Pacific Ocean side is approximately 12 million sq. kms. The surface area of the IPWP undergoes pronounced (50-100%) variability at decadal and longer timescales.

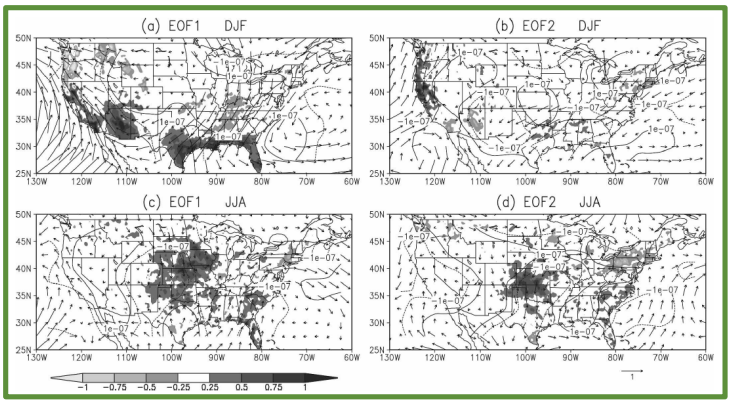

Figure 2: U.S. rainfall (unit: mm day^{-1}, shadings), 850-hPa wind (unit: m s^{-1}, vectors) and divergence (contours) anomalies for (a), (b) DJF and (c), (d) JJA associated with two leading EOFs of the IPWP SST. The maps are linear regressions vs each EOF time series with a two standard deviation departure. Contour value is 1x10^{-7} s^{-1} with negatives dashed and the zero contour omitted.

Decadal variability of the IPWP SST and its association with atmospheric and oceanic circulations were investigated with observed 50-year (1952–2001) SST, and atmospheric and oceanic reanalysis data. It was found (Wang and Mehta, 2008) that two leading empirical orthogonal function patterns (EOFs) well represent the IPWP SST decadal variations. Spatial evolution of EOF1 is dominated by opposing changes in zonal and meridional dimensions and thus a strong deformation of the IPWP on decadal time scales; EOF2 is dominated by changes in size and intensity of the IPWP. Analyses of sub-surface ocean temperatures associated with the two SST EOFs indicated that decadal changes in the IPWP can extend down to 200-300 m depth. Atmospheric circulations and rainfall exhibited substantial responses to the two decadal IPWP SST EOFs over the U.S. (Fig. 2) and in other parts of the world.

We also investigated interannual to decadal variability of the west Pacific Warm Pool (WPWP) and the west Atlantic Warm Pool (WAWP) SSTs and its association with ocean surface variables with remote sensing based 27-yr (1982–2008) Optimal Interpolation SST; 15-yr (1993-2008) sea-surface height (SSH) from TOPEX/Poseidon, Jason-1, and ERS 1/2; 9-yr (1999-2008) surface wind stress (SWS) from QuikScat; and 15-yr (1992-2007) surface current (SC) from Ocean Surface Current Analyses-Real time (OSCAR) data sets. Data products from the 12-yr (1992-2004) Estimating the Circulation and Climate of the Ocean (ECCO) oceanic reanalysis system were also used in this study. During the analysis period, dominant anomalous SST patterns evolved largely *in situ* in the WPWP region, and then moved northeast into north Pacific from the WPWP, possibly transported by the surface branch of the northern sub-tropical cell or the subtropical gyre. SSH and SC variability were physically consistent with SST variability in

some years. A thermally-direct atmospheric response to the WPWP SST anomalies was implied by anomalous SWS convergence over warmer than average SSTs; extra-tropical SWS anomalies were also associated with WPWP SST anomalies, possibly connected via the Hadley circulation and/or Rossby waves to anomalous atmospheric heating in the WPWP region associated with SST anomalies. The SST variability was driven largely by net surface heat flux, especially latent heat flux, with a negligible role of advection terms (Mehta and Wang, 2017a).

In the WAWP at interannual timescales, surface wind stress appears to respond in a thermally-direct manner such that there is anomalous convergence over warmer water. There is also a definite relationship between interannual variability in the WAWP, and eastern and central tropical Pacific. At the decadal time scale, variability of the Atlantic Meridional Overturning Circulation (AMOC) is associated with SSH variability in the tropical Atlantic, such that a bipolar pattern of SSH anomalies from the German ECCO (GECCO) data set, with opposite signs on two sides of the equator, develops 1-2 years after AMOC strength reaches a maximum and persists for several years. The development of a bipolar SST anomaly pattern, however, was not evident in the GECCO data. Substantial SST anomalies developed in the North Atlantic 1-2 years after the AMOC maximum and persisted for several years. Anomalous surface currents from OSCAR show an out-of-phase relationship with WAWP SST anomalies and surface wind stress from QuikScat, suggesting that ocean dynamics are involved in the WAWP SST variability, but a detailed heat budget analysis using ECCO data shows that surface heat fluxes, especially latent heat flux, play the dominant role in interannual SST variability (Mehta and Wang, 2017b).

These results show that the quality of multi-decades long, independently-estimated, remote sensing based ocean surface variables is high enough that a coherent, physical picture of interannual WPWP and WAWP variability can emerge from analyses of these data sets. These results also imply that ocean dynamical processes, in addition to ocean-atmosphere interactions via surface heat flux, are also involved in interannual variability of the TWPs.

2.2 Assessment of Simulations of the Pacific Decadal Oscillation, the tropical Atlantic Sea-surface Temperature Variability, and the West Pacific Warm Pool Variability by the HadCM3, CCSM4, MIROC5, and CM2.1 Earth System Models

The ability of four Earth System Models (ESMs) to simulate major attributes of sea-surface temperature (SST) manifestations of the Pacific Decadal Oscillation (PDO), the tropical Atlantic SST gradient (TAG) variability, and the West Pacific Warm Pool (WPWP) SST variability was assessed. Data from simulation experiments conducted under the CMIP5 project with the CM2.1, HadCM3, MIROC5, and CCSM4 ESMs from 1861 to 2005 were used. A Multi-Model Ensemble was also formed by combining data from the four ESMs. Aerosol optical depths (AODs) and solar radiation were specified in these experiments.

The simulation of PDO spatial pattern, annual cycle, and preferred timescales is the closest to observed attributes in these ESMs. The simulated and observed TAG SST patterns are generally similar, but their average annual cycles are very different and simulated TAG variability does not have a preferred decadal timescale unlike observed variability. Not one of the ESMs is able to simulate the WPWP SST pattern. Simulated and observed average annual cycles of the WPWP SST are similar, and the dominant timescale of WPWP variability is close to 8 years in all ESMs and observations. Simulation skills (defined as correlation coefficients between observed and simulated indices) of the three phenomena fluctuate from decade to decade in all ESMs. Major volcanic eruptions substantially influence observed and simulated indices and simulation skills of the three phenomena. The mixing of net surface heat flux anomalies to 200 m depth in the tropical and mid-latitude Pacific, and the WPWP region causes a delayed and multiyear response of the PDO and WPWP indices to volcanic eruptions as shown in Figure 3 for the WPWP response in the four ESMs (Mehta et al., 2017a).

Composites of AOD and observed WPWP SST anomaly; and anomalous net surface heat flux, SST, and sub-surface ocean temperatures from each of the four ESMs during 3 Volcanic Explosivity Index (VEI) 6 and 4 VEI 4 and 5 events (hereafter referred to as VEI 4+5) led to insights into how and how much these events influenced WPWP SST index. These composites from 12 months before eruption to 60 months

after eruption are shown in Figure 3; note that x-axis scale is the same for all ESMs and variables, but y-axis scales for each variable are not the same for all ESMs due to different sensitivities of the ESMs to AOD changes. In the VEI 6 eruptions, the observed WPWP SST index (Fig. 3, second row) begins to decrease as the AOD begins to build up in the atmosphere approximately 6-8 months before eruption peak. Although variability due to other dynamical forcings increases the WPWP SST index for a few months, the overall decreasing trend continues to 12 months after eruption peak when the index reaches the minimum (-0.28°C) and stays there for 8 months, subsequently increasing in the next 36 to 40 months. The composite, observed WPWP SST index in the VEI 4+5 eruptions shows a general decrease 12 to 20 months after eruption peak, but it is less (-0.1° to -0.2°C) than the decrease for the VEI 6 eruptions; as for the VEI 6 eruptions, effects of other dynamical forcings on the WPWP SST index are evident (Fig. 3, second row). We will see now how each of the ESMs responded to the composite AOD changes.

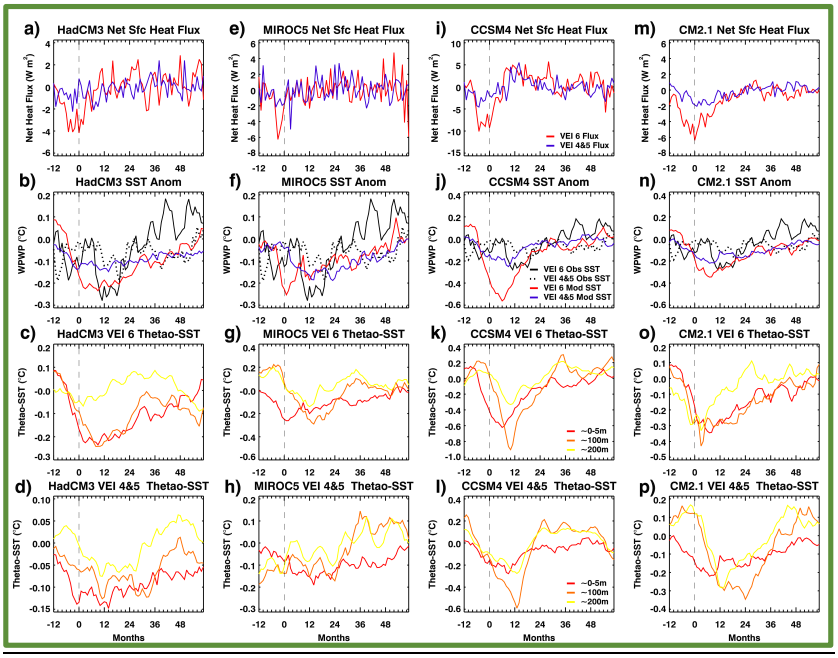

Figure 3: Composite evolutions of net surface heat flux anomalies (Wm^{-2}) averaged in the West Pacific Warm Pool (WPWP) region, observed and simulated WPWP sea-surface temperature anomalies, and sea-surface temperature (0 to 5 m depth) and potential temperature anomalies (°C) at approximately 100 m and 200 m depths averaged in the WPWP region simulated by the HadCM3, MIROC5, CCSM4, and CM2.1 Earth System Models (ESMs) in volcanic eruption events. Monthly anomalies with respect to 1861 to 2005 CE average from 12 months before to 60 months after eruptions, simulated by HadCM3 (boxes a to d), MIROC5 (boxes e to h), CCSM4 (boxes i to l), and CM2.1 (boxes m to p) ESMs, are depicted. Composites contain averages of three eruption events of Volcanic Explosivity Index (VEI) 6 and four eruption events of VEI 4 and 5. Vertical dashed line at 0 month indicates peak eruption time. Legends for each row are shown in boxes i to l. Each ESM's name is shown above each column.

The top row in Figure 3 shows monthly, net surface heat flux anomalies from each ESM, averaged in the WPWP region, from 12 months before to 60 months after composite AOD peaks in VEI 6 and VEI 4+5 events. All ESMs begin responding to AOD increases as eruptions begin and the net surface heat flux anomalies decrease to a maximum negative value approximately 4 months before the AOD peak. The duration and magnitude of the flux decrease varies among ESMs with maximum magnitude (-8 to -10 Wm^{-2}) in CCSM4 (Fig. 3i) and maximum duration (12 to 16 months) in CM2.1 (Fig. 3m) for the VEI 6 eruptions; the largest contribution to net surface heat flux anomalies is by decreasing downward shortwave radiation due to increased albedo. For the VEI 4+5 eruptions, maximum magnitude of decrease (average -3 Wm^{-2}) is in CCSM4 (Fig. 3i) and maximum duration of the decrease (12 to 14 months) is in CM2.1 (Fig. 3m). SSTs and sub-surface ocean temperatures in the ESMs respond to various extents to these net surface heat flux changes. SST decreases begin as the net surface heat flux begins to decrease, but the minimum SSTs are reached 4 to 8 months after AOD peaks, except in MIROC5 the minimum SST

is almost at the time of AOD peak. The SST decreases in VEI 6 eruptions range from -0.2°C in HadCM3 (Fig. 3b) to -0.55° C in CCSM4 (Fig. 3j). Sub-surface temperature anomaly composites for VEI 6 eruptions (Fig. 3, third row), averaged in the WPWP region, show that the volcanic signal is mixed substantially to approximately 200m and then decreases by one or more orders of magnitude at lower depths. This depth of signal penetration is consistent with 150 to 200m mixing depths estimated from anomalous net surface heat flux and time rate of change of temperature shown in Figure 3. In VEI 4+5 eruptions, the depth of substantial penetration of volcanic signal is the same as in VEI 6 eruptions, but the temperature anomalies are smaller (Fig. 3, fourth row). Thus, vertical mixing of heat, forced by reduced net surface heat flux, seems to be the primary driver of WPWP SST response during and after volcanic eruptions. The delay and longer duration of temperature anomalies than those of net surface heat flux are due to vertical mixing of the heat anomaly in the upper ocean. It is interesting to observe in Figure 3 (second row) that although the observed WPWP SST index shows effects of other variability, the underlying cooling of observed index lasts as long as the cooling in the ESM WPWP SST index; the magnitude of the cooling in the ESMs, as mentioned earlier, depends on the net heat flux anomaly generated by each ESM and the response of the ESM's oceanic component to the generated flux anomaly. In the observed WPWP index and in upper ocean ESM temperatures in the WPWP region, the recovery time to average conditions appears to take 4 to 5 years. Thus, VEI 4 and higher explosivity volcanic eruptions clearly and substantially change the phase of the WPWP variability from positive to negative as these results show.

2.3 Assessment of Predictability of the Pacific Decadal Oscillation, the tropical Atlantic Sea-surface Temperature Variability, and the West Pacific Warm Pool Variability by the HadCM3, CCSM4, MIROC5, and CM2.1 Earth System Models

Data from decadal hindcast experiments conducted under CMIP5 were used to assess the ability of CM2.1, HadCM3, MIROC5, and CCSM4 ESMs to hindcast (retrospectively forecast) SST indices of the PDO, the TAG variability, and the WPWP SST variability from 1961 to 2010. As in simulation experiments (Section 2.2), AOD and other external forcings were specified in these experiments, and the ESMs were initialized at specific times with observed data to make 10- and 30-year hindcasts/forecasts.

All ESMs hindcast occurrence frequencies of positive and negative phases of the indices, and probabilities of same-phase transitions from one year to the next reasonably well. Except for the PDO in the 1980s, not one of the decade-average hindcasts show significant skill. Major volcanic eruptions are associated with phase transitions of indices in observed data and in some of the ensemble-average hindcasts. Some phase transitions associated with volcanic eruptions are also present in non-initialized simulations with these ESMs (Section 2.2). Hindcasts from some of the ESMs show correct phase transitions in the absence of AOD changes also, implying that initializations with observed data are beneficial in predicting phase transitions. The best-performing ESM, MIROC5, predicts PDO and WPWP indices to decrease from maxima in 2016 to minima in 2018-19. The skills of PDO and WPWP indices' phase prediction up to at least two years in advance, and perhaps longer, can be used to inform societal impacts management decisions (Mehta et al., 2017b).

2.4 Influences of Net Atmospheric and Riverine Freshwater in Decadal Ocean and Climate Variability

In addition to the observational results described in Section 2.1, modeling and observational studies by other researchers show that the IPWP region is also a "fresh pool" because it receives copious amounts of rainfall and that this can influence IPWP temperature by modifying vertical heat mixing processes and large-scale heat transports. These results strongly suggest that coupled atmosphere-ocean processes may be responsible for interannual-multidecadal variability of the IPWP, in which interactions between upper ocean and the atmosphere via the net atmospheric freshwater flux, defined as evaporation minus precipitation (EmP) at the surface, may be very important. Therefore, the response of the IPWP, and the Pacific and Atlantic Oceans, to EmP at interannual and longer timescales was studied with the Massachusetts Institute of Technology (MIT) ocean general circulation model (OGCM). The OGCM was forced by observed, monthly EmP from 1988 to 2000, derived from evaporation estimates from the Goddard

Satellite Surface Turbulent Fluxes and precipitation estimates from the Global Precipitation Climatology Project; and by climatological heat and momentum fluxes. Observed interannual variations of sea-surface salinity (SSS) in the WPWP were simulated successfully (Fig. 4). Our simulations show (Huang and Mehta, 2004) that the magnitude of interannual anomalies of salinity and temperature reaches about 0.7 psu and 0.4°C, respectively. The typical timescale of these interannual variabilities is about 3 to 5 years. The diagnosed budgets of salinity and temperature (heat) to estimate the role of advection and vertical mixing in response to the surface EmP forcing indicate that the salinity anomaly in the IPWP is largely due to vertical mixing, especially in the surface layer. The vertical mixing of salinity, in turn, is associated with the surface EmP anomaly. In contrast, the temperature anomaly above 300 m is primarily due to changes in advection forced by the EmP, which is associated with basin-wide changes in major ocean currents. Because of the strong effect of advection on the interannual variability of temperature, the temperature anomaly in the surface layer lags the salinity anomaly about 14 to 15 months.

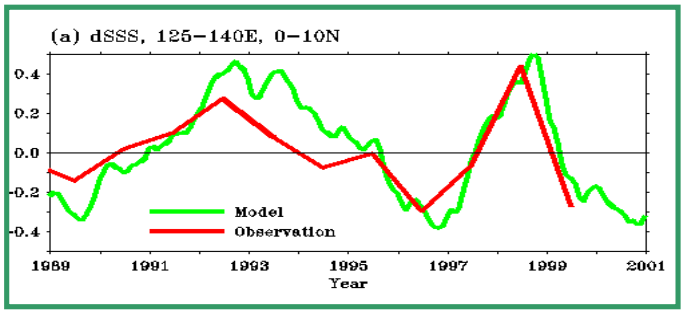

Figure 4: Observed and simulated sea-surface salinity anomalies in the West Pacific Warm Pool.

MIT OGCM simulations also showed (Huang and Mehta, 2005) that the spatial distribution of the average SSS changes during the 1988 to 2000 period in the Pacific and Atlantic Oceans resembled that of average EmP changes, because SSS changes were primarily associated with anomalous vertical mixing forced by the anomalous EmP. The spatial distribution of average near-surface temperature anomalies, however, was different from those of average EmP and SSS anomalies. Analyses indicated that temperature changes in the subtropical North and South Pacific resulted from anomalous heat advection which, in turn, resulted from changes in the subtropical gyre circulations caused by anomalous EmP. Temperature changes in the Atlantic Ocean, however, were largely associated with vertical mixing changes due to anomalous EmP.

To further explore the magnitude of salinity and temperature anomalies and their generation processes in response to EmP anomalies, we studied the response of the Pacific Ocean to idealized EmP anomalies in the tropics and subtropics using the MIT OGCM. Simulations showed (Huang et al., 2005) that salinity anomalies generated by the anomalous EmP were spread throughout the Pacific basin by advection by mean flow. This redistribution of salinity anomalies caused adjustments of basin-scale ocean currents, which further resulted in basin-scale temperature anomalies due to changes in heat advection caused by anomalous currents. The temperature anomalies propagated from the tropical Pacific to the subtropical North and South Pacific via equatorial, divergent Ekman flows and poleward western boundary currents, and they propagated from the subtropical North and South Pacific to the western tropical Pacific via equatorward-propagating coastal Kelvin waves and to the eastern tropical Pacific via eastward-propagating equatorial Kelvin waves. The slower response of ocean temperatures in these simulations due to changes in basin-scale heat advection suggests the possibility that ocean and, perhaps, climate variability, at interannual and longer timescales can be generated by large-scale EmP forcing at seasonal and longer timescales.

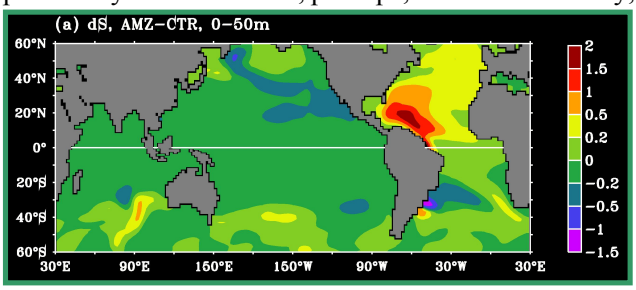

Figure 5: Salinity differences (psu) in the upper 50m between blocked and unblocked Amazon River experiments.

Many large dams on rivers have been built in the last 100 years to store freshwater for societal uses and more large dams are in the offing as the world's thirst for freshwater continues to increase. Not much is known, however, about the possible consequences of blocking the river water flowing into the

world's oceans. Therefore, we have started to study responses of global ocean circulation and temperature to freshwater run-off from major rivers. In the initial simulations, the run-off from several major rivers was selectively blocked in the MIT OGCM. Run-offs into the tropical Atlantic, the western North Pacific, and the Bay of Bengal and northern Arabian Sea were selectively blocked, using monthly river run-off data from the world's major rivers. The blocking of river run-off first resulted in a significant (2 psu) salinity increase near the river mouths (e.g., Fig. 5 for the Amazon River blocking). The saltier and, therefore, denser water was then transported to higher latitudes in the North Atlantic, North Pacific, and southern Indian Ocean by mean currents. The subsequent density contrasts between Northern and Southern Hemisphere oceans resulted in changes in major ocean currents. These anomalous ocean currents led to significant temperature changes (1-2ºC) by the resulting anomalous heat transports. The current and temperature anomalies created by the blocked river runoff propagated from one ocean basin to others via coastal and equatorial Kelvin waves. This initial study (Huang and Mehta, 2010) suggests that river runoff may be playing an important role in oceanic salinity, temperature, and circulations; and that partially or fully blocking major rivers to divert freshwater for societal purposes might significantly change ocean salinity, circulations, temperature, and atmospheric climate.

2.5 Estimation of the Fundamental Global Water Cycle Using Satellite Remote Sensing Data

The understanding and prediction of local, regional, and global water cycles are very important for understanding and prediction of societal impacts of water, especially water availability for domestic and industrial uses, and agriculture. There is substantial progress in understanding local and regional water cycles; but global water cycles, their variability, and changes are poorly quantified and understood. A major reason for this lack of progress is the non-availability of long-term observations of evaporation, precipitation, and water vapor transport, especially over the oceans. Among all global-scale water cycles, the most important one is the fundamental global water cycle (FGWC), defined as the annual cycle of evaporation, precipitation, and water vapor transport between the Northern and Southern Hemispheres.

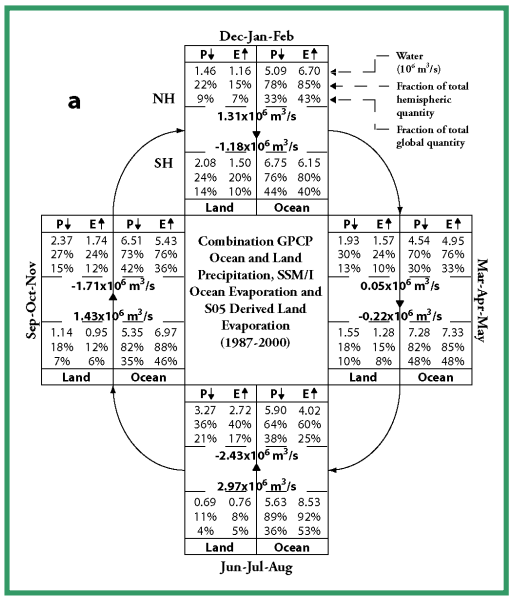

Figure 6: The FGWC based on precipitation, GSSTF2 over-ocean evaporation, and over-land evaporation based on combined S05 EmP and GPCP precipitation during 1988-2000. Arrows and numbers across the hemispheric interface denote the direction and amount of net moisture flux transport. All quantities are in units of 10^6 m^3/s.

We quantified the average FGWC over 13 years with remote-sensing-based precipitation estimates from the Global Precipitation Climatology Project (GPCP) Version 2 data sets and over-ocean evaporation estimates from the Goddard Satellite Surface Turbulent Fluxes Version 2 data set from 1988 to 2000. Over-land evaporation was estimated from the remote-sensing-based precipitation estimates combined with a global evaporation minus precipitation (EmP) data set. Results show (Mehta et al., 2005) that 75% to 85% of the total global evaporation and approximately 70% of the total global precipitation occurs over the oceans in each season. In the GPCP-based FGWC estimate, there is a remarkable balance in the inter-hemispheric import-export of atmospheric moisture in December-January-February and June-July-August seasons. The dominant cross-equatorial atmospheric water vapor transports in the atmospheric branch of the FGWC supply a significant amount of moisture to precipitation regions and are from the Northern Hemisphere to the Southern Hemisphere in December-January-February and the Southern Hemisphere to the Northern Hemisphere in June-July-August, with approximately $3x10^6$ m^3 s^{-1} net annual transport from the Southern Hemisphere to the Northern Hemisphere in the GPCP-based FGWC estimate (Fig. 6). These unique results show that evaporation,

precipitation and atmospheric water vapor transport over the oceans play a very important role in the FGWC and that they should be a significant component in national and international research programs on the global water cycle.

3. Research on Societal Impacts of Natural Decadal Climate Variability

3.1 Decadal Climate Variability Impacts on Run-off and River Flows in the Missouri River Basin

It is well-known that weather and climate variability cause substantial impacts on freshwater resources. With demands on water resources increasing due to several reasons, it is very important to understand and predict, if possible, weather and climate impacts on freshwater. There have been several studies of impacts of El Niño-Southern Oscillation and global warming on water resources in the U.S., but the study of impacts of natural DCV on water resources are in their infancy. Therefore, we began a systematic program of study in 2006 to assess DCV impacts on water resources and predict the impacts if possible. We began with the Missouri River Basin (MRB) because it is the largest river basin in the U. S., is one of the most important crop and livestock-producing regions in the world, and experiences a pronounced decadal variability of dry and wet epochs (Fig. 7). Results from this program are briefly described.

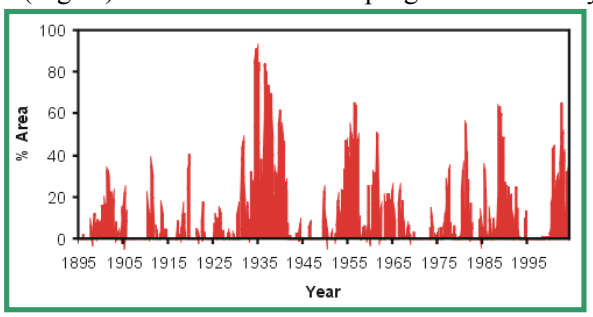

Figure 7: Percent of total Missouri River Basin area experiencing severe to extreme drought between January 1895 and March 2004. Based on data provided by the National Climatic Data Center, NOAA; Copyright 2004 National Drought Mitigation Center.

In an exploratory study of associations between observed DCV phenomena and hydro-meteorological (HM) variability in the MRB for Northern Hemisphere spring and summer, it was found that positive and negative phases of the PDO, the TAG variability, and the WPWP variability were significantly associated with decadal variability in precipitation and surface air temperature, with combinations of various phases of these DCV phenomena associated with dry, wet, or neutral HM conditions. As an example, Figure 8 shows precipitation and daily maximum temperature anomaly patterns associated with positive and negative phases of the PDO. These patterns were derived with regression analyses of observed precipitation and PDO index data from 1961 to 2010 (Mehta et al., 2011a, 2016).

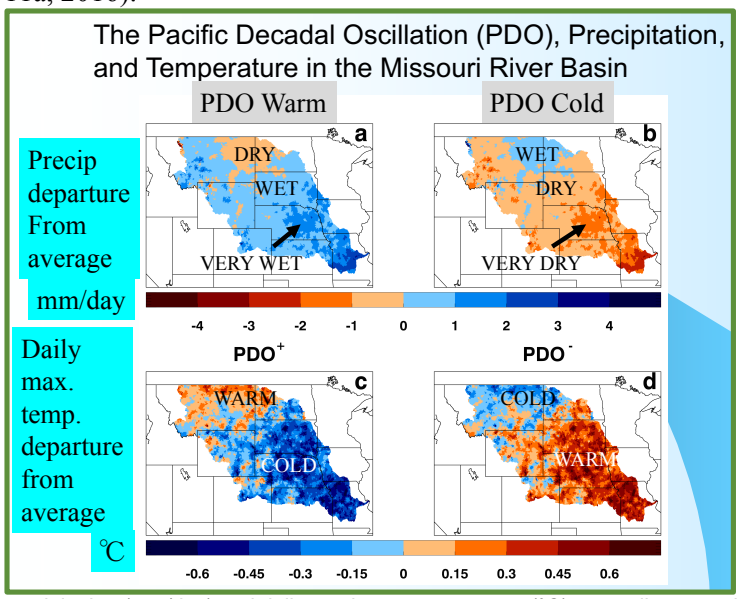

Figure 8: Annual-average precipitation (mm/day) and daily maximum temperature (°C) anomalies associated with (a) PDO^+, precipitation, (b) PDO^-, precipitation, (c) PDO^+, temperature, and (d) PDO^-, temperature. Color scales for each variable are shown below each row.

Figures 8a and 8c show that in the positive or warm phase of the PDO, almost the entire MRB is wetter and cooler than average; the climate is drier and warmer in the northern part of the Basin in this PDO phase. In the negative or cold PDO phase, much of the MRB is drier and warmer than average (Figs. 8b and 8d), with the northern part wetter and cooler than average.

To simulate impacts of DCV on water run-off and river flows and predict them, we developed and applied methodologies to two versions of the land use-hydrology-crop model Soil and Water Assessment Tool (SWAT). In the exploratory study (Mehta et al., 2011a), we used the Hydrologic Unit Model of the United States (HUMUS) – SWAT version, calibrated and validated for the MRB. HUMUS-SWAT was applied at 75 widely-distributed, 8-digit hydrologic unit areas within the MRB. HUMUS-SWAT driven by HM anomalies in both the positive and negative phases of the PDO and TAG resulted in substantial impacts on water run-off; impacts of the WPWP were smaller. For all three DCV indices, the simulated impacts on water yield at the 75 study sites were approximately consistently distributed throughout the region (Mehta et al., 2011a).

We then applied this experimental methodology to a fine-scale version of SWAT which included a crop growth module. This version of SWAT was highly calibrated and validated (Daggupati et al., 2016) for the MRB in 11 land use classes such as wheat belts, rangeland areas, corn and soybean belts, forests and pasturelands, mixed agricultural and pasture lands, sand dunes and rangelands, and forests. The fine-scale MRB SWAT includes land use – land cover information at 30 m resolution, crop rotation and irrigation. It also includes irrigated land and soil data; and precipitation, temperature, winds, solar radiation data at 12 km x 12 km. The calibration process included crop yield calibration for winter and spring wheat, dryland and irrigated corn, and dryland and irrigated soybeans. The water yield calibration was done for total surface and base flows. The SWAT calibration did not include water abstractions and other human-made changes. Three types of experiments were conducted with SWAT: (Type I) With daily or monthly, observed HM data as input from 1961 to 2010; (Type II) with idealized HM data based on DCV scenarios as input; and (Type III) with decadal HM hindcasts from 1961 to 2010, derived from either a hybrid dynamical-statistical technique or from downscaled Earth System Model (ESM) hindcasts. In each type of SWAT experiments, water and crop yields and streamflow outputs were compared with appropriate observed data (NASS crop yields and USGS streamflow). We also developed a statistical crop yield and river flow prediction technique using past, observed data. Figure 9 shows a schematic diagram of the three types of SWAT experiments.

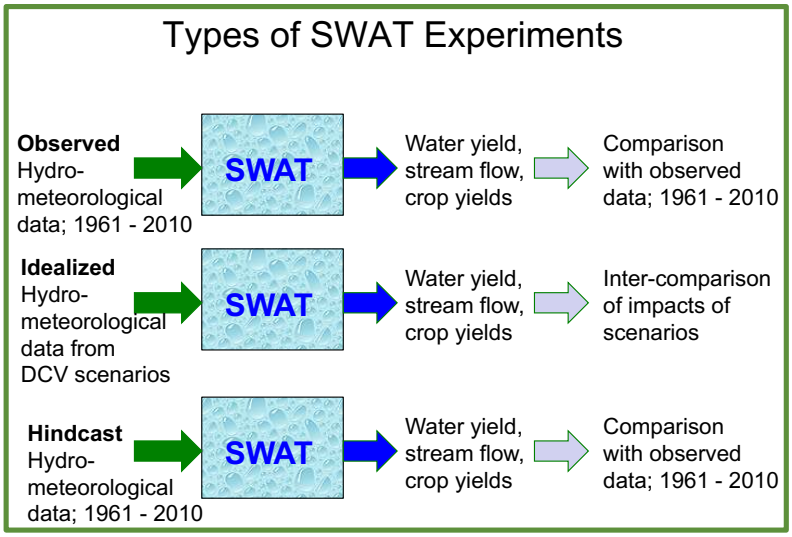

Figure 9: SWAT experiments with observed, idealized, and hindcast hydro-meteorological data.

SWAT was then applied at approximately 14,000 watersheds (each with 12 km x 12 km area) to estimate impacts on run-off, river flows, and other water variables in response to realistic values of PDO, TAG, and WPWP variability. We simulated impacts of each individual DCV phenomenon and its phases as well as combinations of DCV phenomena's phases. As an example, Figure 10 shows SWAT-simulated water yield anomalies (surface and groundwater run-off anomalies) in response to an idealized scenario (Type I experiment) of PDO-associated HM anomalies shown in Figure 8. In PDO-only scenarios, water yield (Fig. 10a) increased by 10%–30% of average yield in most of the MRB in response to forcing anomalies associated with the positive PDO phase (Figs. 8a, c), but not in eastern and western Montana, western North Dakota, and individual locations in South Dakota, Nebraska, Colorado, and Wyoming, where the yield decreased by 10%–20%. In response to forcing anomalies associated with PDO- (Figs. 8b, d), water yield (Fig. 10b) decreased almost everywhere by 10%–20%, except for some isolated locations in Montana, North and South Dakota, Wyoming, Colorado, and Nebraska. The average water yield change over the entire MRB in both phases of the PDO was within ±20% of average yield.

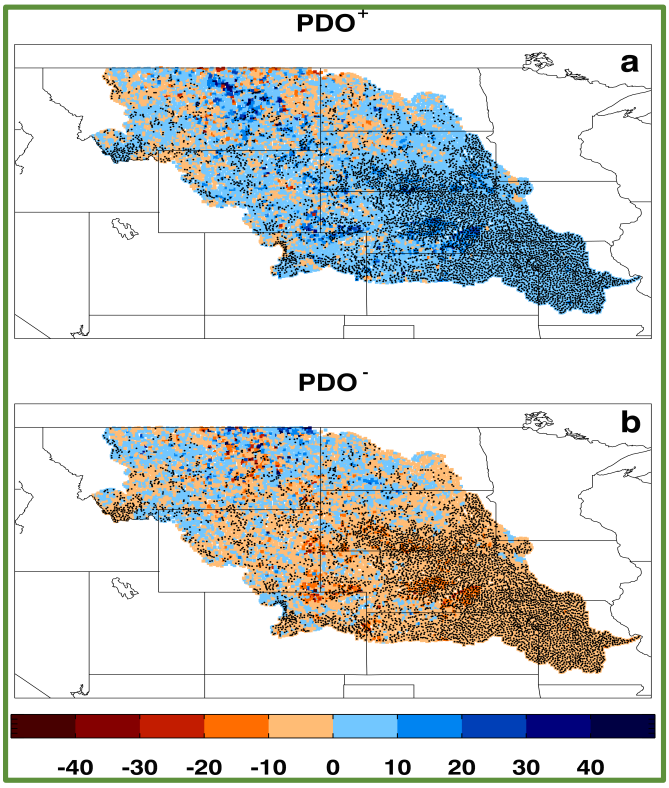

Figure 10: SWAT-simulated annual-average water yield (% change from climatology) in the MRB in (a) PDO^+ and (b) PDO^- phases. Black dots show locations of 95% significance.

In general, physical agreement with the PDO-associated precipitation and temperature anomalies in Figure 8, USGS-observed river flow anomalies in a specific warm PDO period (1982-1986) (Fig. 11a, left column) were positive in almost the entire MRB, implying above average flows. In a specific cold PDO period (1987-1990), river flow anomalies were negative in almost the entire MRB (Fig. 11a, right column); that is, river flows were below average in this period. In a Type II experiment, SWAT simulated river flows during these two PDO periods reasonably well as Figure 11 shows. Figures 11b (left and right columns) show the simulated river flow anomalies in these two periods, which are very similar to the USGS-observed river flow anomalies. Thus, observed HM and river flow data, and simulated river flows show substantial impacts of the PDO in the MRB. The TAG variability and other DCV phenomena make smaller but significant impacts on the MRB as well (Mehta et al., 2016).

SWAT, driven by HM anomalies associated with positive and negative phases of PDO and TAG in Type II experiments, indicated major impacts on water yields and river flows, as much as 40% of the average in many locations; impacts of the WPWP variability were smaller. Consistent with observations during 1949–2010, SWAT showed water flow increases of as much as 80% of the average, causing very wet epochs when positive phase of the PDO and negative phase of the TAG at extreme amplitudes were superposed. Water flows decreased by a similar amount, resulting in severe to extreme droughts, when negative phase of the PDO and positive phase of the TAG at extreme amplitudes were superposed (Mehta et al., 2016). Thus, the SWAT experiments show that combined and cumulative effects of these DCV phenomena on run-off, river flow, and dry and wet epochs in the MRB can be dramatic, with important consequences for all water-consuming sectors as well as for feedbacks to the climate system.

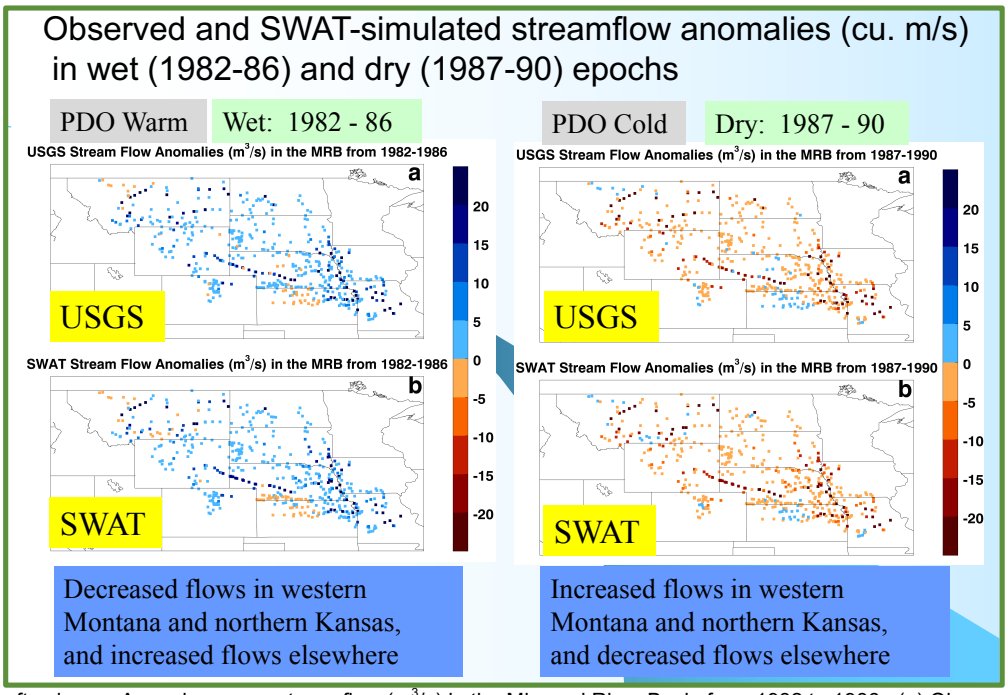

Figure 11: Left column: Annual-average streamflow (m^3/s) in the Missouri River Basin from 1982 to 1986. (a) Observed USGS estimate, (b) simulated SWAT estimate. Right column: Annual-average streamflow (m^3/s) in the Missouri River Basin from 1987 to 1990. (a) Observed USGS estimate, (b) simulated SWAT estimate.

3.2 Decadal Climate Variability Impacts on Crop Yields in the Missouri River Basin

It is well-known that weather and climate variability cause substantial impacts on agriculture. With demands on food production increasing due to several reasons, it is very important to understand and predict, if possible, weather and climate impacts on crop production. As in the case of water resources, there have been several studies of impacts of El Niño-Southern Oscillation and global warming on crop production in the U.S. and other countries, but the study of impacts of natural DCV on crop yields are in their infancy. Therefore, we began a systematic program of study in 2006 to assess DCV impacts on crop yields and production. We began with the MRB because, as mentioned in Section 3.1, it is the largest river basin in the U. S., is one of the most important crop and livestock-producing regions in the world, and experiences a pronounced decadal variability of dry and wet epochs. Results from this program are briefly described.

Impacts of the dry and wet epochs shown in Figure 7 on spring and winter wheat production aggregated in the MRB can be seen in Figure 12 in which production estimates by the U.S. Department of Agriculture's National Agricultural Statistics Service (NASS) from 1961 to 2010 are shown along with the PDO index for the same period. Correlation coefficients between each of the wheat production time series and the PDO index time series are approximately 0.5 (at least 95% significance) without smoothing and

0.65 after smoothing the time series. As is clear from Figure 12, there are very substantial, multiyear to decadal variations – compared to the 50-year average - in wheat production. The TAG index has a smaller correlation with MRB wheat production, but its associations with wheat production anomalies in some epochs are unmistakable. Not only climate variability, but also market forces and government policies influence crop production and, therefore, a perfect correlation cannot be expected with any of these and other drivers of crop production. The associations between the PDO and TAG indices and wheat production in the MRB, however, are clearly apparent in observed data. These associations - in conjunction with DCV-related atmospheric winds, water vapor transport, precipitation, and temperature in the MRB (Mehta, 2017) - provide a strong motivation to simulate and predict DCV impacts on the production of wheat and other crops in the MRB.

To begin with, we used the Erosion Productivity Impact Calculator (EPIC; also known as Environmental Policy Integrated Climate) model, calibrated and validated for the MRB, to simulate yields of non-irrigated corn, winter and spring wheat, and soybean in response to HM anomalies associated with the aforementioned DCV phenomena. This exploratory study in which EPIC was run at 75 locations in the MRB showed that HM anomalies associated with realistic values of DCV indices can make major impacts on crop yields, as much as 50% of average yield in some locations in the MRB; however, our results also showed that the impacts can be location-specific. The results of this study are described in Mehta et al. (2012).

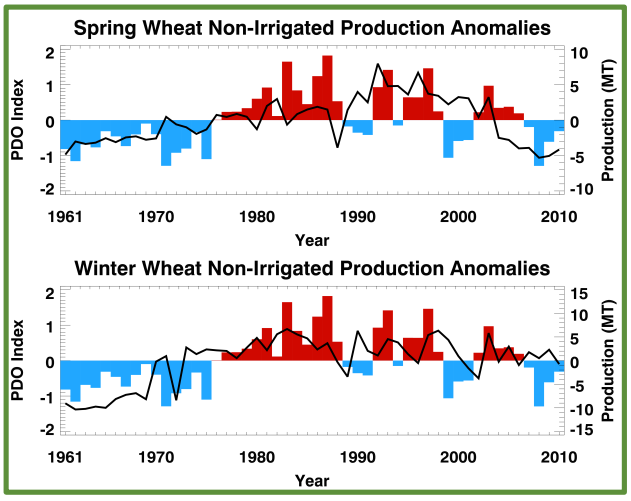

Figure 12: Wheat production anomalies (bars; million tons; right scale) aggregated in the Missouri River Basin and the Pacific Decadal Oscillation index (black line; left scale) from 1961 to 2010. The average spring and winter wheat productions in this period were 6.63 million tons and 13.8 million tons, respectively.

The Type II simulation experiments with the fine-scale SWAT, mentioned in Section 3.1, indicated major impacts of PDO and TAG phases with average amplitudes on wheat yields, as much as ±40% of the average in many locations; spring and winter wheat yield changes in positive phase of the PDO are shown in Figure 13. Impacts of the WPWP index variability were smaller, but no less substantial. Consistent with observations during the 1950 to 2010 period, SWAT showed wheat yield increases of 40% causing abundant production when positive phase of the PDO and negative phase of the TAG were superposed. Wheat yields decreased by a similar amount resulting in a significantly lower production when negative phase of the PDO and positive phase of the TAG were superposed.

In general, physical agreement with the PDO-associated precipitation and temperature anomalies in Figure 8, NASS-estimated winter wheat yield anomalies in a specific warm PDO period (1982-1986) (Fig. 14a, left column) are positive in almost the entire MRB, implying above average yields. In a specific cold PDO period (1987-1990), winter wheat yield anomalies were negative in almost the entire MRB (Fig. 14a, right column); that is, yields were below average in this period. In a Type I experiment, SWAT

simulated winter wheat yields during these two PDO periods reasonably well as Figure 14 shows. Figures 14b (left and right columns) show the simulated yield anomalies in these two periods, which are very similar to the NASS-estimated yield anomalies. Thus, observed HM and winter wheat yield data, and simulated winter wheat yields show substantial impacts of the PDO in the MRB. The TAG variability and other DCV phenomena make smaller but significant impacts on the MRB crop yields as well (Mehta et al., 2017c).

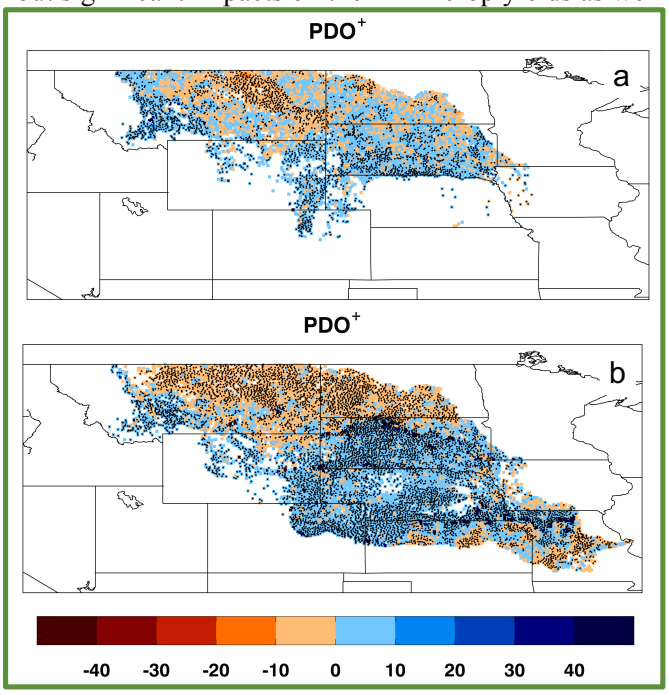

Figure 13: SWAT-simulated annual-average wheat yields (% change from long-term average) in the Missouri River Basin in using average amplitudes in positive phase of the Pacific Decadal Oscillation (PDO^+). (a) Spring wheat, (b) winter wheat. Black dots show locations of 95% significance.

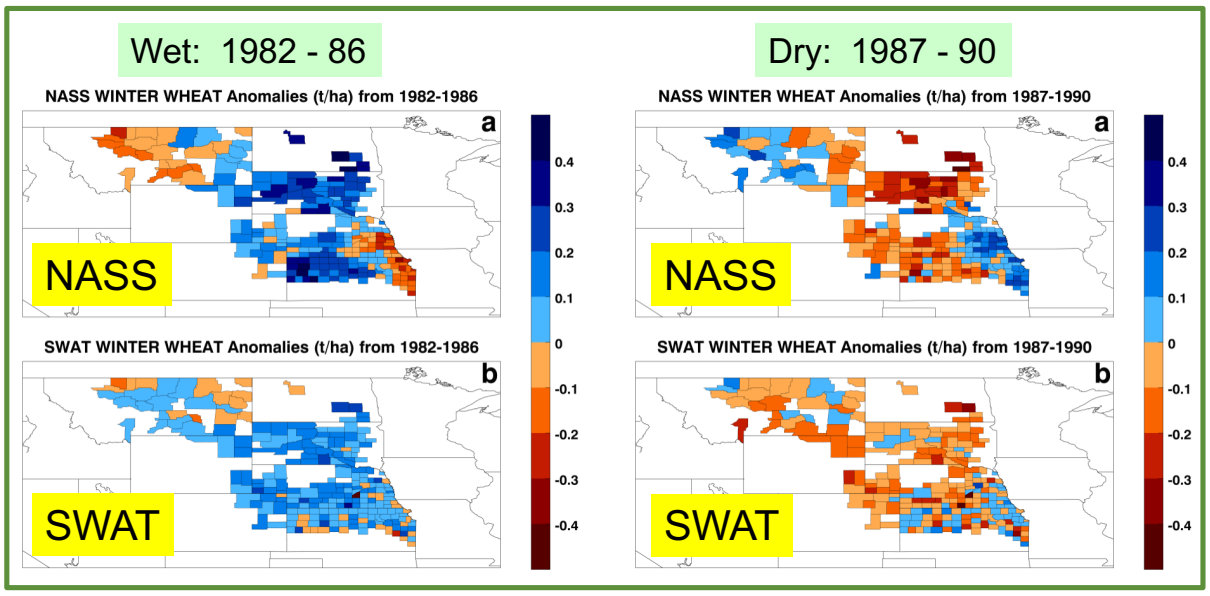

Figure 14: A comparison of annual SWAT-simulated and NASS-estimated winter wheat yield anomalies.

SWAT, driven by HM anomalies associated with positive and negative phases of PDO and TAG, indicated major impacts on yields of major crops, as much as 40% of the average in many locations; impacts of the WPWP variability were smaller. Consistent with observations during 1949–2010, SWAT showed crop yield increases of as much as 80% of the average, causing abundant crop productions when the positive phase of the PDO and the negative phase of the TAG at extreme amplitudes were superposed. Crop productions decreased by a similar amount, resulting in very low productions, when the negative phase of the PDO and the positive phase of the TAG at extreme amplitudes were superposed (Mehta et al., 2016).

These results show that DCV impacts can influence decisions from the farm to the national level, including in commodity trading. Thus, the combined and cumulative effects of these DCV phenomena on crop yields and productions in the MRB can be dramatic, with important consequences for local, regional, and national economies; and national and international food securities.

3.3 Experimental Prediction of Impacts of the Pacific Decadal Oscillation and the tropical Atlantic Sea-surface Temperature Gradient Variability on Yields of Wheat, Corn, Soybeans, Alfalfa, and other Crops in the Missouri River Basin; and Development of Adaptation Options

Using the insights in DCV impacts on MRB agriculture, the fine-scale version of SWAT, and the expertise in using county-wise NASS data on yields of major crops in the MRB which we gained in research described in Section 3.2, we are developing techniques to predict crop yields in selected sub-basins within the MRB. The selected sub-basins are the Central (or Middle) Platte in Nebraska, the Lower Grand straddling Missouri and Iowa, the James straddling North and South Dakota, and the Marias in Montana. These sub-basins were selected because of their major crops' sensitivity to DCV and are shown in Figure 15.

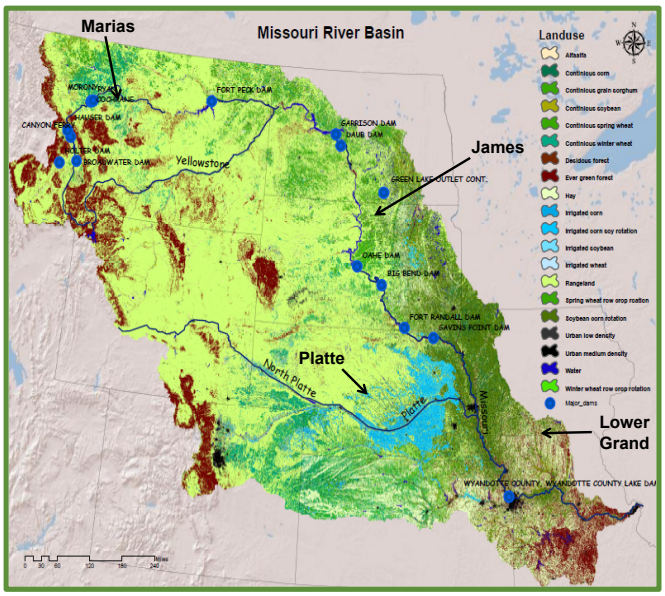

Figure 15: Selected sub-basins for development of prediction and adaptation options.

As described in Section 3.1, we conducted three types of experiments with SWAT to develop the simulation and prediction system. Since the observed HM data can be considered "perfect" forecasts, results of Type I experiments imply that SWAT can be considered a reasonably accurate prediction system for impacts of HM variability on river flow and crop yields in the MRB. Type II SWAT experiments with idealized, DCV-associated HM scenarios were used to test the sensitivity of water and crop yields to DCV phenomena and to predict these yields for a given prediction of DCV phases and magnitudes. In Type III experiments, SWAT was forced by hindcast HM data to make hindcasts of river flows and crop yields. In addition, using NASS crop yield data from 1961 to 2010, we developed statistical models of yields of major

crops in each county, linking crop yield anomalies to positive and negative phases of the PDO, the TAG variability, and the WPWP variability. These statistical models were also used to predict crop yields based on prediction of phases of these three DCV phenomena with ESMs.

For each crop, we used the three prediction techniques described in Section 3.1 and the statistical prediction technique, in conjunction with ESM-based DCV index prediction described in Section 2.2. Only a few examples of crop yields prediction in two sub-basins are shown here to illustrate successful applications of the techniques. Figure 16 shows winter wheat yield anomaly prediction in the 9 counties of the Platte River sub-basin in two epochs, a wet epoch associated with positive PDO phase in 1982 to 1984 and a dry epoch associated with negative PDO phase in 1988 to 1990. We used hindcast of the PDO made with the MIROC5 ESM which was initialized January 1981 and run for 10 years. For example, for the 1982-84 yield prediction, we used the 1982-84 ensemble-average PDO hindcast made by MIROC5. Since the MIROC5 prediction was for positive PDO phase, we selected the average wheat yield anomaly in each county, calculated from the 1961-1980 NASS estimates, as the 1982-84 yield prediction. Based on the MIROC5 PDO hindcast, we selected the SWAT-simulated wheat yield anomalies as the hindcast. Wheat yield hindcasts for the 1988-90 period were made in a similar way. Figure 16a shows wheat yield prediction made for the 1982 to 1984 wet epoch with the statistical model, Figure 16b shows prediction made with the SWAT model (Type II experiments described in Section 3.1), and Figure 16c shows the actual (NASS) winter wheat yield in this epoch. Figure 16d shows wheat yield prediction made for the 1988 to 1990 dry epoch with the statistical model, Figure 16e shows prediction made with the SWAT model, and Figure 16f shows the actual (NASS) winter wheat yield in this epoch.

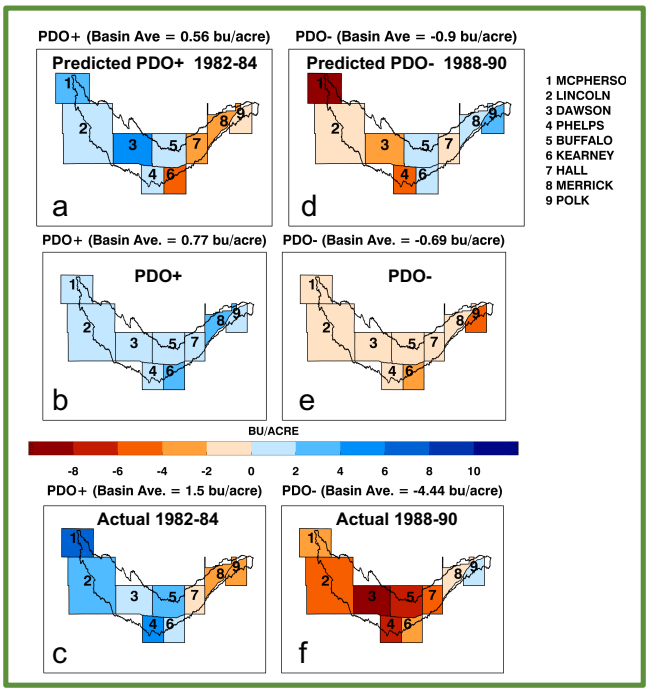

Figure 16: Multiyear to decadal prediction of winter wheat yield anomalies in the Platte River sub-basin. See text for details.

Figures 16a-b-c show that both statistical model and SWAT-based techniques predicted the correct sign of the wheat yield anomalies (above average) in the western part of the sub-basin in the wet epoch whereas the statistical model based technique also predicted the below-average yield anomalies in the eastern part of the sub-basin. In the dry epoch also (Fig. 16d-e-f), while both statistical model and the SWAT-based technique generally predicted below-average yield anomalies, above-average yield anomalies were predicted correctly in the eastern part of the sub-basin only by the statistical model. Although the magnitude prediction by both techniques was not accurate, it must be emphasized that these predictions

were started in 1981 and are truly multiyear to decadal predictions. Further research will focus on more accurate magnitude prediction.

One of the major crops in the Marias sub-basin is barley, so we show here barley prediction with the statistical and SWAT models with the techniques described above and the MIROC5 hindcast of the PDO initialized in 1981 and run for 10 years. Figure 17 shows barley yield anomaly prediction in the 10 counties of the Marias sub-basin in the 1982 to 1984 wet epoch and the 1988 to 1990 dry epoch. Figure 17a shows barley prediction made for the 1982 to 1984 wet epoch with the statistical model, Figure 17b shows prediction made with the SWAT model, and Figure 17c shows the actual (NASS) barley yield anomalies in this epoch. Figures 17d-e-f show the corresponding barley yield anomalies in the 1988 to 1990 dry epoch. As for the Platte River sub-basin wheat prediction, Figures 17a-b-c show that both statistical model and SWAT-based techniques predicted the correct sign of the barley yield anomalies (above average) in much of the Marias sub-basin, in this case the southern part in the wet epoch whereas neither technique predicted the below-average yield anomalies in the northern part of the sub-basin. In the dry epoch (Fig. 17d-e-f), while both statistical model and the SWAT-based technique generally predicted below-average yield anomalies, the SWAT-based technique performed much better in predicting correctly below-average yield anomalies in the central and northern parts of the Marias sub-basin.

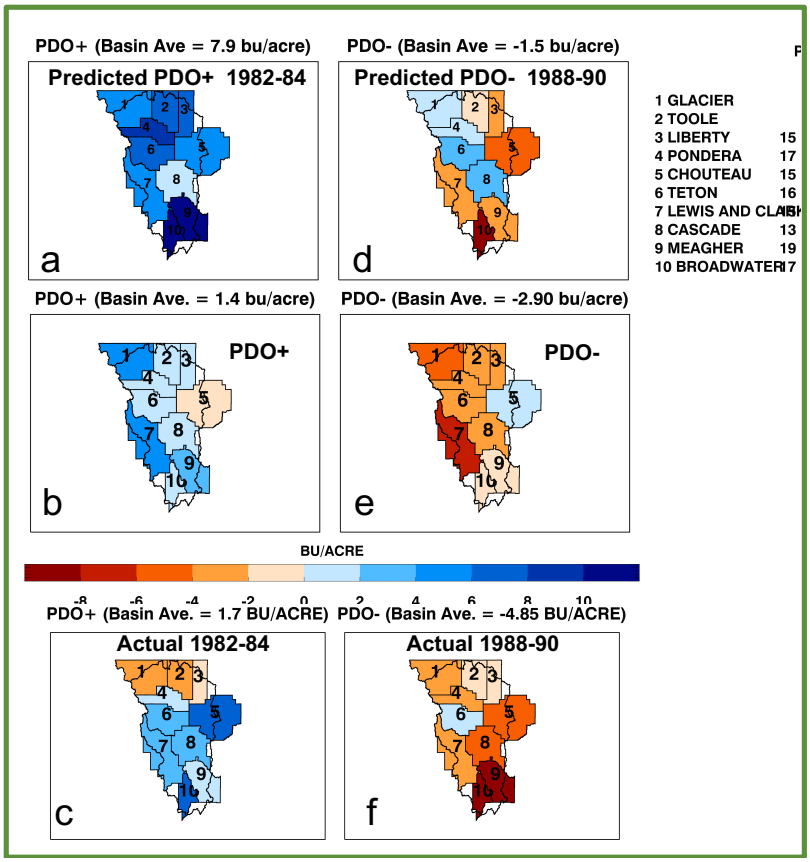

Figure 17: Multiyear to decadal prediction of barley yield anomalies in the Marias sub-basin. See text for details.

Thus, these two cases of sub-basin and crop combinations show that the models and methodologies we are developing are successful in multiyear to decadal prediction of crop yield anomalies. Of course, this success is dependent on the ability of ESMs to skillfully predict at least the sign of the DCV indices. However, the DCV sign prediction is not always successful several years in advance and so more research effort is needed.

Based on the crop simulation and prediction models and methodologies we developed, and webinars and workshops with members of the Stakeholder Advisory Teams, a crop adaptation methodology was developed. An example for the Platte River sub-basin is described here. Corn, hay, soybeans, and winter wheat are the major crops in this sub-basin within the MRB. Changes in magnitudes of their yields are associated with various combinations of DCV phases. In the example described here, the associations between two DCV phase combinations – (PDO^+, TAG^-) and (PDO^-, TAG^+) – and crop yields (Fig. 18) are used to generate adaptation information for farmers in the Platte River sub-basin. As Figure 18 shows, the probability of an above-average yield of corn and hay is much higher than the probability of a below-average yield of these two crops in the (PDO^+, TAG^-) combination, whereas the probabilities of below-average soybeans and winter wheat yields is much higher. Thus, it would be beneficial for farmers in most of the Platte River sub-basin counties to plant corn or hay in this DCV phase combination. In the (PDO^-, TAG^+) phase combination, it would be beneficial for farmers to plant soybeans in almost the entire sub-basin rather than corn, hay, or winter wheat because the probabilities of an above-average soybeans yield are much larger than the probabilities of below-average soybeans yield.

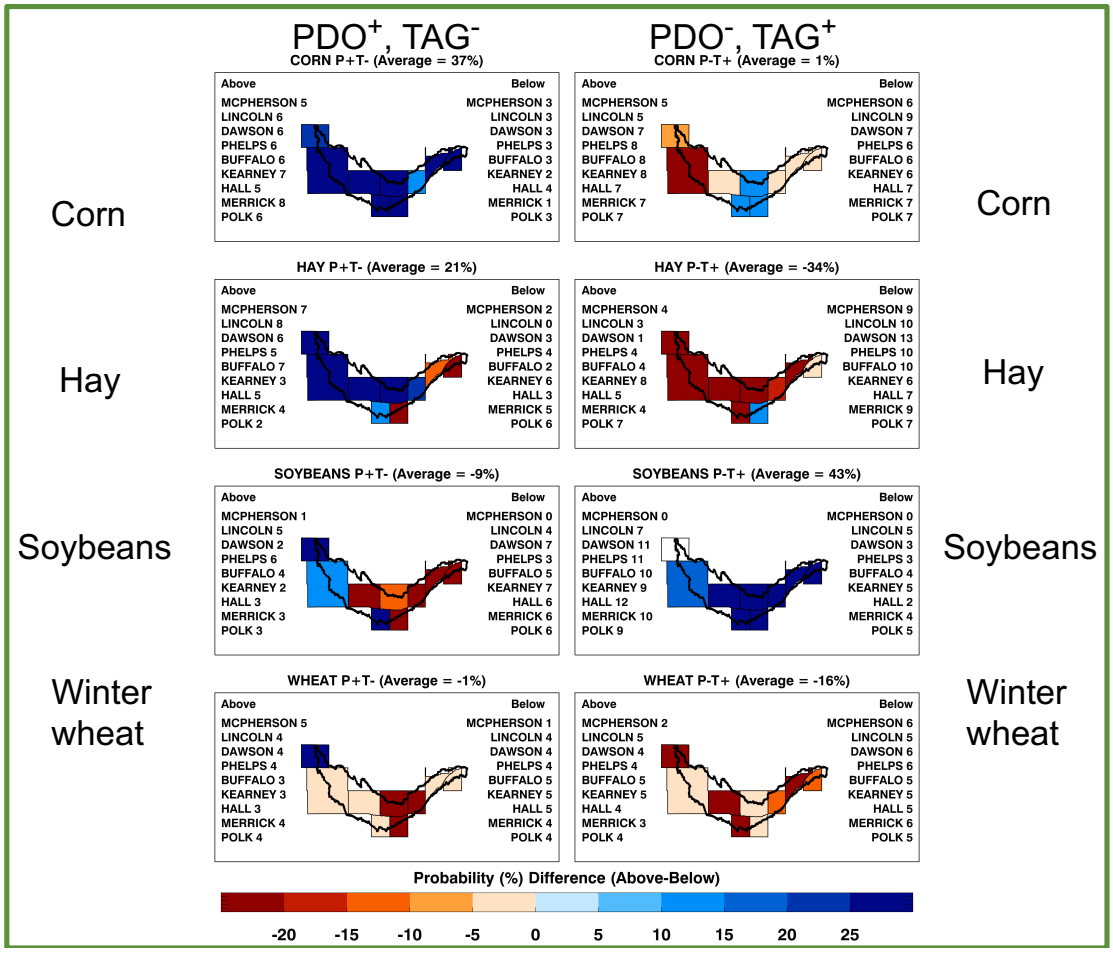

Figure 18: An example of adaptation options for farmers in two predicted DCV phase combinations in the Platte River sub-basin. See text for details.

3.4 Assessments of Decadal Drought Information Needs of Stakeholders and Policymakers in the Missouri River Basin for Decision Support

As mentioned earlier in the report, the MRB is the largest river basin in the U.S., and decadal droughts and wet epochs in the MRB are correlated with various combinations of the three DCV

phenomena. With collaborators from the National Drought Mitigation Center, University of Nebraska – Lincoln, and the Institute for Water Resources, U.S. Army Corps of Engineers, we have been working since 2006 on assessing impacts of DCV phenomena and stakeholder information needs in the MRB for decision support with respect to decadal dry and wet epochs. This has been done through: (1) workshops involving stakeholders in the Basin; (2) development of retrospective dry and wet epoch scenarios with respect to DCV phenomena and their associations with HM variables in the Basin; and (3) development of sectoral impact evaluations through use of the HUMUS-SWAT, EPIC, and SWAT models driven by the retrospective scenarios.

Approximately 100 stakeholders in the MRB, representing the water and agriculture sectors have helped define the problems and research approach we have developed. This has been accomplished by means of eight dedicated workshops and many webinars as well as interviews and discussions with well-placed individuals. There was a unanimous agreement among stakeholders that there are identifiable and quantifiable impacts, including economic impacts, of DCV on water, including urban water security, and agriculture. They made many important and specific suggestions to climate scientists for providing DCV information. Participants experienced DCV impacts on water and agriculture in the past and know that credible climate information can be useful in their work. The stakeholders are eager (e.g., Fig. 19) to use climate information, including decadal climate outlooks, as and when available. But, there are obstacles to the effective use of such information by stakeholders: credibility of climate information must be established; institutional rules and regulations must be addressed and laws and legal precedents developed. The results of these assessment workshops and individual discussions are summarized in Rosenberg et al. (2007) and Mehta et al. (2013, 2016, 2017c).

Figure 19: Honorable John Bohlinger, Lt. Governor of Montana, explaining the importance of CRCES's societal impacts research to Workshop participants in Helena, Montana, in 2009.

3.5 Impacts of the Pacific Decadal Oscillation, the tropical Atlantic Sea-surface Temperature Variability, and the West Pacific Warm Pool Variability on the Mississippi River Transportation System

On the 41,009 km (25,482 miles) of navigable inland waterways in the U.S., approximately 650 million tons of cargo and over 2 million twenty-foot equivalent unit containers valued at over $75 billion are transported every year. These cargo and containers are transported by over 30,000 barges of various types. There are 28 inland ports that handle over 250,000 short tons of cargo every year. Agricultural products are the main cargo shipped, with corn, soybean, and wheat making up a large percentage of the total. Other major cargoes include coal, raw materials (including sand, gravel, iron ore, and scrap iron), manufactured products, petroleum products, and chemicals. Much of the agricultural cargo is destined for export through ports on the Gulf of Mexico. Grain corn accounts for approximately 10-12% of all U.S. agricultural exports, which is 50-60% of global corn exports. The U.S.'s shares of the world's wheat and soybean exports are approximately 20% and 40%, respectively. Sixty percent of all grain exported from

the U.S. is shipped on the Mississippi River from its main production regions in the MRB and Mississippi River Basin (MsRB) to the Port of New Orleans and the Port of South Louisiana on the Gulf of MexicoTherefore, representing 500 million tons of shipped cargo per year, the Mississippi River barge port system is significant to national and international trade and food security. In order to keep the Mississippi and other inland waterways navigable, the U.S. Army Corps of Engineers spends approximately $1.5 billion per year for dredging the waterways. Therefore, it is very important to assess and understand impacts of weather and climate variability on inland, water-borne transportation systems.

The DCV phenomena which impact hydro-meteorology and river flows in the MRB also impact them in the MsRB as shown in Figures 20a-d for the PDO and Figures 21a-d for the TAG variability.

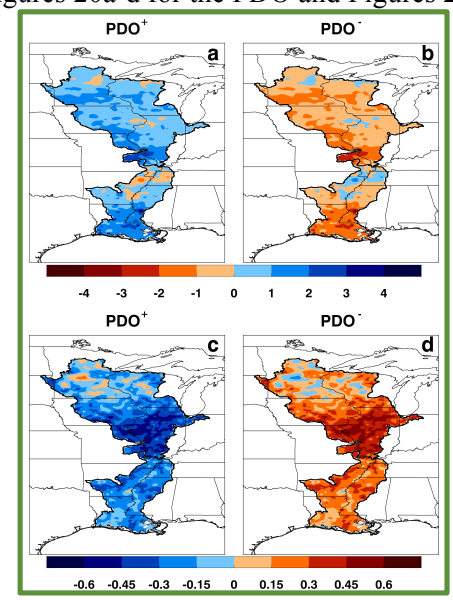

Figure 20: Precipitation (mm/day) and daily maximum temperature (°C) anomalies associated with positive and negative phases of the Pacific Decadal Oscillation at average amplitude. (a) Precipitation in PDO^{+}, (b) precipitation in PDO^{-}, (c) temperature in PDO^{+}, and (d) temperature in PDO^{-}. Color scales are shown below each row.

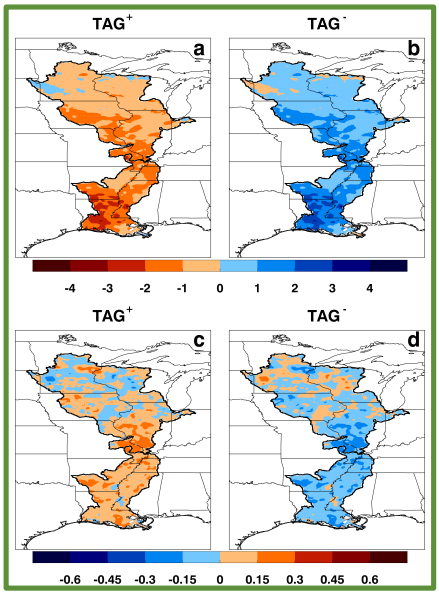

Figure 21: Precipitation (mm/day) and daily maximum temperature (°C) anomalies associated with positive and negative phases of the tropical Atlantic SST gradient (TAG) variability at average amplitude. (a) Precipitation in TAG^{+}, (b) precipitation in TAG^{-}, (c) temperature in TAG^{+}, and (d) temperature in TAG^{-}. Color scales are shown below each row.

As Figures 20a and 20b show, there is above- and below-average precipitation in the MsRB in positive and negative phases of the PDO, respectively, by several mm/day. Figures 20c and 20d show that daily maximum temperatures are cooler and warmer by 0.15° to 0.45°C in positive and negative phases of the PDO, respectively. These figures indicate that there are wetter and cooler conditions in positive phase of the PDO and dryer and warmer conditions in negative phase of the PDO. Generally opposite conditions exist during positive and negative phases of the TAG variability as Figures 21a-d show. Variability of the West Pacific Warm Pool (WPWP) sea-surface temperatures (SSTs) and El Niño-La Niña events also have substantial associations with MsRB hydro-meteorology.

The Middle Mississippi River (MMR) is the segment of the Mississippi River from the confluence with the Missouri River near St. Louis, Missouri, to the confluence with the Ohio River near Cairo, Illinois – a distance approximately 320 km (200 miles). Approximately 120 million tons of cargo is shipped on the MMR each year. Agricultural products are the main cargo, with corn, soybean, and wheat making up a large percentage of the total. Much of the agricultural cargo is destined for export through ports on the Gulf of Mexico. There are no locks or dams downstream of St. Louis to maintain water levels, so inland navigation on this stretch of the Mississippi River is vulnerable to natural flow variations and, therefore, navigation on this stretch of the Mississippi River is perhaps the most vulnerable to natural flow variations due to climate variability. Dikes, bank revetments, and dredging are used to maintain a navigable channel in the MMR.

Figure 22 shows observed DCV indices, river flows in the MMR and elsewhere in the MsRB, cargoes transported on the MMR, and dredging volume. Based on these and other data, an ensemble of case studies of high- and low-flow epochs using empirical data was developed to aid quantitative analyses. A descriptive analysis method is a better approach rather than a purely statistical analysis method when inter-relationships among processes and impacts, as represented in empirical data, may be physically consistent but not statistically stationary. Also, hydro-meteorology and agriculture are impacted by several DCV phenomena simultaneously, so there may not be a stationary statistical relationship with any one phenomenon. Moreover, crop yields, productions, and prices may suffer both in low and high precipitation epochs; water-borne transportation may suffer both in high- and low-flow epochs; and dredging may be required both in high- and low-flow epochs, but the timing of the dredging may be different in the two epochs. Therefore, a descriptive approach was adopted in diagnosing possible connections among DCV phenomena, precipitation and temperature, river flow, crop production, water-borne transportation, and dredging. The analyses consisted of visual inspections of data time series and assembly of "word pictures" of sequences of events from DCV to hydro-meteorology to river flow; and to crop production, transportation, and dredging. Reasonably detailed, but only for some years, information about the Mississippi waterway operations, and types and numbers of vessels used at ports on the Mississippi River are available from the USACE for some of these prominent epochs and they were also included to make the "word pictures" more complete.

Based on time series of Mississippi River flow at St. Louis and other locations along the Mississippi and Missouri Rivers, the following periods of high and low flows were selected as case study epochs. The high-flow/flood years are 1993-94 and 2008-11. The low-flow/drought years are 1987-89, 2000, 2003-06, and 2012-13. Cargo transportation data are not available before 1988, therefore only wet/dry epochs beginning in 1988 are described. All four high-flow epochs at St. Louis occurred during the negative phase of the TAG variability which is associated with above-average precipitation, below-average temperature, and above-average river flow in the MRB and the MsRB. The PDO was either in the positive phase or had a small negative amplitude; the former is associated with above-average precipitation, below-average temperature, and above-average river flow in the MRB and the MsRB. During most of the six low-flow epochs at St. Louis, the TAG variability was in the positive phase and/or the PDO and Niño3.4 were in the negative phase; these phases are associated with below-average precipitation, above-average temperature, and below-average river flow. Thus, specific phases of the DCV phenomena were associated with the 10 high-flow and low-flow epochs. Two of these case studies are shown here in Figures 23 and 24.

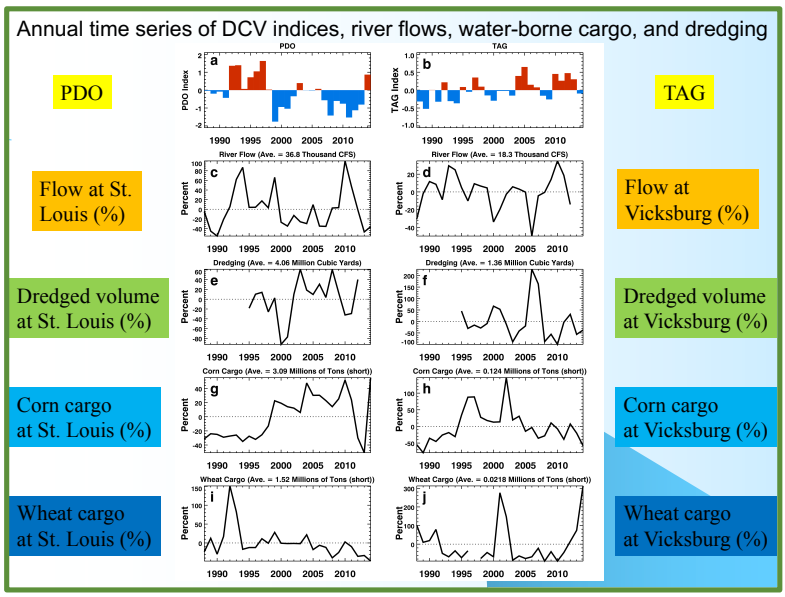

Figure 22: Annual time series of (a) the Pacific Decadal Oscillation, (b) the tropical Atlantic sea-surface temperature gradient, (c) Mississippi River flow anomalies (%) at St. Louis, (d) Mississippi River flow anomalies (%) at Vicksburg, (e) dredged volume anomalies (%) at St. Louis, (f) dredged volume anomalies (%) at Vicksburg, (g) corn cargo anomalies (%) at St. Louis, (h) corn cargo anomalies (%) at Vicksburg, (i) wheat cargo anomalies (%) at St. Louis, and (j) wheat cargo anomalies (%) at Vicksburg. The 1988-2014 average value is given above each box from c to j.

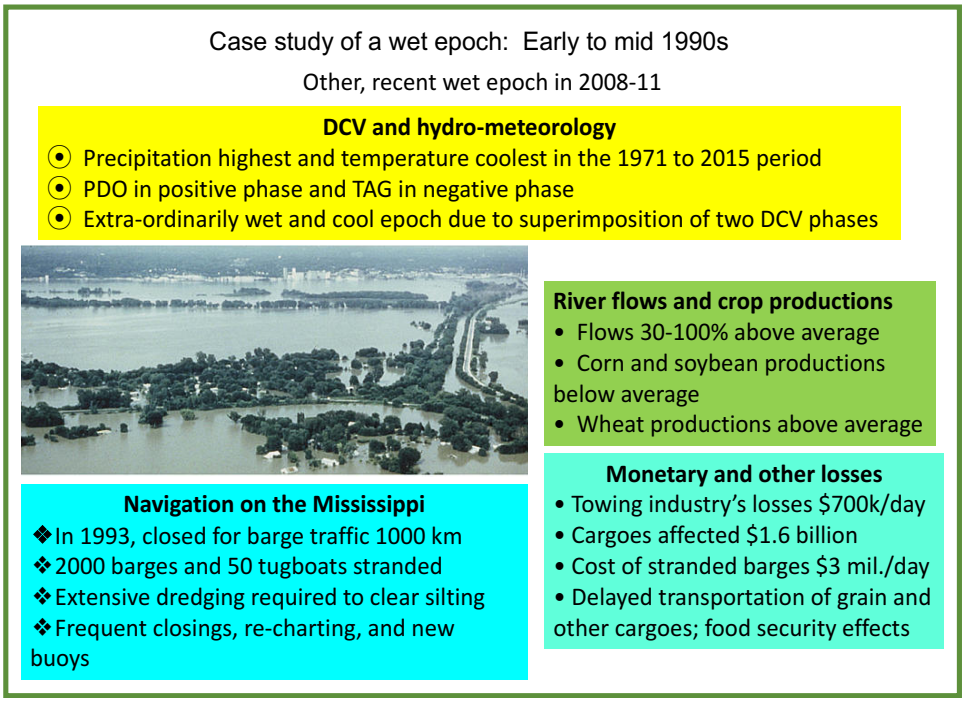

Figure 23: A case study of impacts on water-borne transportation in a wet epoch in early to mid 1990s in the Mississippi River Basin.

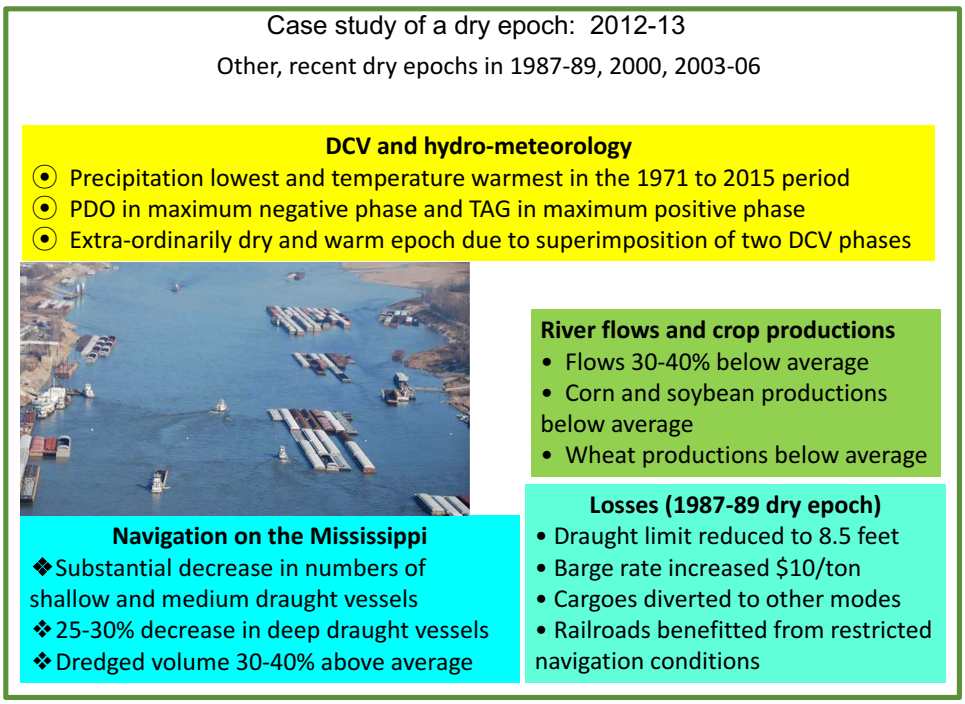

Figure 24: A case study of impacts on water-borne transportation in a dry epoch in 2012-13 in the Mississippi River Basin.

3.6 Decadal Climate Variability and Urban Water Security

An exploratory study of impacts of interannual to decadal climate variability on urban water security in three case-study areas, and mail survey of over 700 urban water systems of various sizes was conducted. Substantial impacts of interannual to decadal climate variability on urban water security were found in three small (Great Falls, Montana), medium (Lincoln, Nebraska), and large (Kansas City, Kansas and Missouri) case-study areas. Impacts of climate variability occurred on supply, demand, and access. The degree of impacts was dependent on location with respect to water source, size of supply need, and effectiveness of conservation measures. Municipal water demand was also found to be clearly affected by precipitation and temperature. The PDO was found to impact even electricity cost for pumping water and chemical cost for treating water in Great Falls, Montana, where such data are available. Reasonable success was achieved in predicting probabilities of future climate impacts on urban water supply several seasons in advance, based on past data of local precipitation and temperature in the case-study areas. SWAT forced with observed HM anomalies showed substantial sensitivity of water yields in the case study areas to DCV as found in other areas in the MRB. The simulations also showed a reasonable agreement between observed water consumption and other associated variables in Great Falls and Lincoln areas, and SWAT-simulated water variables. During dry epochs, there were substantial increases in water demand and voluntary or mandatory water restrictions had to be applied; during wet epochs, there were substantial decreases in water demand and increases in water rates charged to customers.

Our mail survey showed that 33-50% of the water systems which responded (over 125 out of 700 systems surveyed) use longer term climate outlooks for planning future water storage needs, expanded distribution systems, justifying infrastructure investments, bringing on new water supplies, adjusting reservoir levels, scheduling personnel, making budget projections, implementing water restrictions, and initiating public information campaigns for water conservation. Over 40% of the respondents said that they are likely to use 1- to 2- year climate outlooks for making budget projections, justifying infrastructure investments, implementing water restrictions, and informing the public on water conservation; 20-25% said that they are likely to use 1- to 2- year climate outlooks for adjusting reservoir levels or planning expanded distribution systems. The most beneficial information for decision-making would be seasonal and 1- to 2-

year outlooks of above- or below- normal precipitation and temperature. Water system managers are interested in using climate information in their decision-making process if such information is available.

3.7 A Hybrid Technique for Decadal Hydro-meteorological Prediction

A cross-validated regression technique was developed for decadal HM predictions. Coefficients of a regression equation between an observed, dependent variable such as precipitation or Palmer Drought Severity Index (PDSI) at each grid point of a geographical grid; and observed indices of the PDO, the TAG, the WPWP, and the Niño 3.4 were estimated using data from 1961 to 2010, with cross-validation based on one decade's data at a time. The regression equation was then used to predict the dependent variable at each grid point using hindcast/forecast DCV indices from the MIROC5 ESM. This technique was first tried for decadal PDSI prediction in southern Africa and showed increasing skill (correlation coefficient and root-mean-square error between observed and predicted PDSI) from the 1960s to the 2000s **(**Figure 25**;** Mehta et al., 2014**)**. This hybrid prediction technique is now being used to make fine-scale HM predictions for the MRB, which will be used to drive fine-scale SWAT to make water and crop yields predictions.

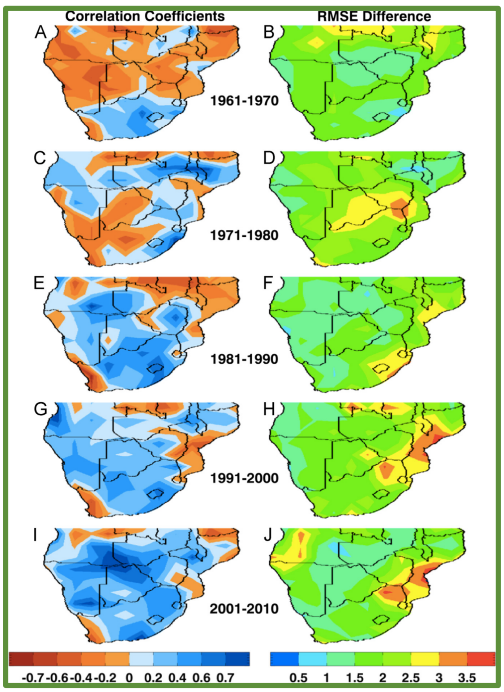

Figure 25: Correlation coefficients and root-mean-square differences between actual and hindcast PDSI from 1961 to 2009–2010, averaged over the October–March rainy season at 2.5º longitude–2.5º latitude grid spacing in southern Africa. Color scales are shown below the figure. The thresholds for significance of correlation coefficients are +/-0.63 for 95%, +/-0.55 for 90%, +/-0.49 for 85%, +/-0.44 for 80%, and +/-0.40 for 75%.

4. Education of Undergraduate and Graduate Students

Collaborations among CRCES, Texas A & M University (TAMU), and University of Maryland – Baltimore County (UMBC) have facilitated the involvement of 5 Ph.D. and 16 undergraduate students in CRCES's projects. Important details of the students' research and training are given here.

Titles of Ph.D. Dissertations:

1. Climate Variability, Water and Agricultural Production; TAMU
2. Decadal Climate Variability: Economic Implications in Agriculture and Water in the Missouri River Basin; TAMU
3. Economic and Societal Implications of Decadal Climate Variability and Fishery Management; TAMU
4. Decadal Climate Variability Impacts on Crop Distributions; TAMU

5. Bayesian and an Expectation – Maximization–Like Estimation of a Tobit State-space Model for Daily Precipitation; UMBC

Under the National Science Foundation (NSF)'s Research Experiences for Undergraduates (REU) Program, hosted by the Interdisciplinary Program in High Performance Computing at UMBC, 16 undergraduate students were involved in CRCES's projects. These students worked on various aspects of CRCES's projects in analyzing HM data from four global ESMs run under the World Climate Research Program's Coupled Model Inter-comparison Project 5, developing statistical techniques to downscale the ESMs' HM data using parallel computing, and developing a web portal for interactive analysis and visualization of the data. Through the REU program, CRCES projects have been instrumental in exposing these undergraduate researchers to complexities of climate modeling, and in training them in climate data processing and analysis.

5. A Leadership Role in Decadal Climate Variability and Societal Impacts Community Development

Beginning with its founding in 2002, CRCES has played a leadership role in the U.S. community of researchers studying DCV and its predictability, and has contributed in important ways to the development of a worldwide community of researchers on this subject. Since 2006, CRCES has also played a leadership role in the U.S. and international communities of researchers studying societal impacts of DCV. To date, CRCES has organized 14 workshops on DCV and/or its societal impacts (workshops are listed in Appendix 2). Financial support from NASA, NOAA, NSF, USDA-NIFA, USGS, and the USDOE facilitated these workshops. The number of participants in these workshops varied from 40 to 125. Most of the workshops focused on DCV and its predictability led to formulation of "white papers" with recommendations to U.S. funding agencies and climate research organizations about DCV research; some of these have been published in the peer-reviewed literature (e.g., Mehta et al., 2006, 2011b). Thus, these workshops have played an important role in developing national and international research programs on DCV. CRCES scientists have also contributed to community-wide "white papers" about DCV and predictability presented in international conferences such as OceanObs99 (Mehta and Latif, 2001) and World Climate Conference 3 (Murphy et al., 2009). To further generate ideas and recommendations about assessment and possible prediction of impacts of DCV in the U.S. on water resources, agriculture, transportation, coastal preparedness, health, insurance industry, and economy, CRCES organized a special workshop to focus on societal impacts of DCV. This workshop brought together a selected and unique group of climate scientists and societal impacts specialists. A "white paper" containing recommendations from this workshop was published by Rosenberg et al. (2007). Reports on the stakeholder interactions workshops are available from missouri.crces.org/publications/reports.

CRCES is also contributing significantly towards international development of climate and societal impacts research, education, and applications. For this purpose, CRCES and the Nirma University of Science and Technology in Ahmedabad, India, organized a workshop titled "The Workshop on Monsoon Climate Variability and Change, and Their Impacts on Water, Food, and Health in Western India" in February 2007. This workshop was co-sponsored by the U.S. NSF and the Indian Government Department of Science & Technology. This workshop brought together over 45 scientists from India, the U.S, Europe, and Japan. Conclusions and recommendations from this workshop led in August 2008 to the founding of the Indian Centre for Climate and Societal Impacts Research (ICCSIR) in Ahmedabad. CRCES scientists were closely involved in the development of ICCSIR and its programs for the first five years.

Soon after its inception, CRCES was one of the pioneers of the application of contemporary information technology to climate research. The community of researchers interested in DCV and its societal impacts is worldwide. Because of the Internet and associated technologies, it is no longer necessary to physically co-locate researchers in one building in order to tackle the immense problems of understanding and prediction of DCV and its impacts. Therefore, with NASA sponsorship, CRCES created "the Virtual Center for Decadal Climate Variability" (Mehta et al., 2006). The DecVar system used the Internet to allow

any participating scientist to do research as if he/she were physically located in a research center--to perform data analysis, communicate with other scientists, and access publications.

The accomplishments briefly described above positioned CRCES as a leading institute in the global decadal climate and societal impacts research communities.

6. Publications

The research described in this Report has already been or is being published as peer-reviewed papers in frontline scientific journals such as *Journal of Geophysical Research-Oceans*; *Journal of Geophysical Research-Atmospheres*; *Journal of Climate*; *Journal of Physical Oceanography*; *Bulletin of the American Meteorological Society*; *Eos – Transactions of the American Geophysical Union*; *Advances in Atmospheric Sciences*; *Journal of the American Water Resources Association*; *Agricultural and Forest Meteorology*; *Weather, Climate, and Society; Journal of Hydrometeorology*; and *Climate Dynamics*. CRCES has also issued special reports about describing specific activities in which it has engaged. CRCES scientists have given invited and contributed seminars and presentations in various national and international conferences and workshops. The list of peer-reviewed publications is given in Appendix 1.

7. Grants, Personnel, and Collaborations

In its first decade and a half, CRCES has obtained multi-million dollars in grants from NASA, NOAA, NSF, USGS, USDOE, USDA–NIFA, and U.S. Army Corps of Engineers-Institute for Water Resources. These grants were awarded for research on DCV analysis, modeling, and predictability studies; global water cycle; assessments of DCV impacts on water resources and agriculture; assessments of decadal drought information needs of stakeholders and policymakers for decision support; development of an experimental decadal climate and impacts prediction system and climate-adaptive water and agriculture management system; assessment of DCV impacts on inland, water-borne transportation systems; assessment of readiness of transportation and agriculture sectors to cope with decadal droughts; and for organizing workshops on DCV and its societal impacts. These grants support senior scientists, research associates, research assistants, information technology specialists, an administrative officer, and infrastructure and administrative expenses. In view of the highly multi-disciplinary nature of CRCES's work, collaborations have been developed with distinguished scientists, public participation specialists, and graduate students with complementary expertise in other organizations. These collaborators and organizations are Drs. Mike Hayes and Cody Knutson, Ms. Nicole Wall, Ms. Tonya Bernadt, and Ms. Tonya Haigh in the National Drought Mitigation Center, University of Nebraska–Lincoln; Drs. Rolf Olsen and Harvey Hill, and Ms. Andrea Carson in the Institute for Water Resources, the U.S. Army Corps of Engineers; Drs. Raghavan Srinivasan, Bruce McCarl, Prasad Daggupati, Debjani Deb, J. Ding, M. Fernandez, P. Huang, and T. Jithitikulchai in Texas A & M University; and Dr. Amita Mehta and Mr. S. Popuri in NASA-University of Maryland at Baltimore County–Joint Center for Earth System Technology.

Appendix 1: CRCES's Peer-reviewed Publications

24. Mehta, V.M., and H. Wang, 2017a: Interannual Variability of Tropical Warm Pools in Remote Sensing Based and ECCO-assimilated Oceanographic Data Sets. Part I: The West Pacific Warm Pool. *J. Geophys. Res.-Oce.*, in preparation.
23. Mehta, V.M., and H. Wang, 2017b: Interannual Variability of Tropical Warm Pools in Remote Sensing Based and ECCO-assimilated Oceanographic Data Sets. Part II: The West Atlantic Warm Pool. *J. Geophys. Res.-Oce.*, in preparation.
22. Mehta, V.M., K. Mendoza, P. Daggupati, N.J. Rosenberg, and R. Srinivasan, 2017c: High-resolution Simulations of Decadal Climate Variability Impacts on Dryland Crop Yields in the Missouri River Basin with the Soil and Water Assessment Tool (SWAT): Spring and Winter Wheat. *Global Change Biology*, in review.
21. Mehta, V.M., H. Wang, and K. Mendoza, 2017a: Simulation of Major Decadal Climate Variability Phenomena in CMIP5 Experiments with the HadCM3, GFDL-CM2.1, NCAR-CCSM4, and MIROC5 Global Earth System Models. *Climate Dynamics*, in review.
20. Mehta, V.M., H. Wang, and K. Mendoza, 2017b: Predictability of Major Decadal Climate Variability Phenomena in CMIP5 Experiments with the HadCM3, GFDL-CM2.1, NCAR-CCSM4, and MIROC5 Global Earth System Models. *Climate Dynamics*, in review.
19. Fernandez, M.A., P. Huang, B. McCarl, and V.M. Mehta, 2016: Value of decadal climate variability information for agriculture in the Missouri River Basin. *Climatic Change*, **139**, 517-533. DOI 10.1007/s10584-016-1807-x.
18. Mehta, V.M., K. Mendoza, P. Daggupati, R. Srinivasan, N. J. Rosenberg, and D. Deb, 2015: High-resolution Simulations of Decadal Climate Variability Impacts on Water Yield in the Missouri River Basin with the Soil and Water Assessment Tool (SWAT). *J. Hydrometeorology*, **17**, 2455 - 2476.
17. Daggupati., P., D. Deb, R. Srinivasan, D. Yeganantham, V. M. Mehta, and N. J. Rosenberg, 2016: Spatial calibration of hydrology and crop yields through parameter regionalization for a large river basin. *Journal of the American Water Resources Association*, **52**, 648 - 666.
16. Mehta, V.M., H. Wang, K. Mendoza, and N.J. Rosenberg, 2014: Predictability and Prediction of Decadal Hydrologic Cycles: A Case Study in Southern Africa. *Weather and Climate Extremes*, **3**, 47-53.
15. Mehta, V.M., H. Wang, and K. Mendoza, 2013: Decadal predictability of tropical basin-average and global-average sea-surface temperatures in CMIP5 experiments with the HadCM3, GFDL-CM2.1, NCAR-CCSM4, and MIROC5 global earth system models. *Geophysical Research Letters*, **40**, doi:10.1002/grl.50236.
14. Mehta, V.M., C. L. Knutson, N. J. Rosenberg, J. R. Olsen, N. A. Wall, T. K. Bernadt, and M. J. Hayes, 2013: Decadal Climate Information Needs of Stakeholders for Decision Support in Water and Agriculture Production Sectors: A Case Study in the Missouri River Basin. *Weather, Climate, and Society*, **5**, 27-42.
13. Mehta, V.M., N. J. Rosenberg, K. Mendoza, 2012: Simulated Impacts of Three Decadal Climate Variability Phenomena on Dryland Corn and Wheat Yields in the Missouri River Basin. *Agricultural and Forest Meteorology*, **152**, 109-124.
12. Mehta, V., G. Meehl, L. Goddard, J. Knight, A. Kumar, M. Latif, T. Lee, A. Rosati, and D. Stammer, 2011b: Decadal Climate Predictability and Prediction: Where Are We? *Bulletin of American Meteorological Society*, **92**, 637-640.
11. Mehta, V.M., N. J. Rosenberg, K. Mendoza, 2011a: Simulated Impacts of Three Decadal Climate Variability Phenomena on Water Yields in the Missouri River Basin. *Journal of the American Water Resources Association*, **47**, 126-135.
10. Huang, B., and V.M. Mehta, 2010: Influences of Freshwater from Major Rivers on Global Ocean Circulation and Temperatures in the MIT Ocean General Circulation Model. *Advances in*

*Atmospheric Sci*ences, **27**, 455-468.

9. Murphy, J., V. Kattsov, N. Keenlyside, M. Kimoto, G. Meehl, V. Mehta, H. Pohlmann, A. Scaife, and D. Smith, 2009: Towards Prediction of Decadal Climate Variability and Change. An invited White Paper for World Climate Conference 3, Geneva.
8. Wang, H., and V.M. Mehta, 2008: Decadal Variability of the Indo-Pacific Warm Pool and Its Association with Atmospheric and Oceanic Variability in the NCEP–NCAR and SODA Reanalyses. *Journal of Climate*, **21**, 5545-5565.
7. Rosenberg, N. J., V. M. Mehta, J. R. Olsen, H. von Storch, R. G. Varady, M. J. Hayes, and D. Wilhite, 2007: Societal adaptation to decadal climate variability in the United States: CRCES workshop on societal impacts of decadal climate variability in the United States. *Eos – Transactions American Geophysical Union*, **88**, 444.
6. Mehta, V., Y. Kushnir, J. Lean, D. Legler, R. Lukas, A. Proshutinsky, N. Rosenberg, H. von Storch, P. Schopf, and W. White, 2006: The CRCES workshop on decadal climate variability. *Bulletin of American Meteorological Society*, **87**, 1223-1225.
5. Mehta, V.M., E.J. Lindstrom, L. de Kort, and A.J. DeCandis, 2006: The Virtual Center for Decadal Climate Variability. *Bulletin of the American Meteorological Society*, **87**, 421-424.
4. Huang, B., V.M. Mehta, and N. Schneider, 2005: Oceanic response to idealized net atmospheric freshwater in the Pacific at the decadal timescale. *Journal of Physical Oceanography*, **35**, 2467-2486.
3. Huang, B., and V.M. Mehta, 2005: The response of the Pacific and Atlantic Oceans to interannual variations in net atmospheric freshwater. *Journal of Geophysical Research-Oceans*, **110**, C08008, doi: 10/1029/2004JC002830.
2. Mehta, V.M., A. J. DeCandis, and A. V. Mehta, 2005: Remote sensing based estimates of the fundamental global water cycle, Part I: The annual cycle. *Journal of Geophysical Research-Atmospheres,* **110**, D22103, doi: 10.1029/2004JD005672.
1. Huang, B., and V.M. Mehta, 2004: The response of the Indo-Pacific Warm Pool to interannual variations in net atmospheric freshwater. *Journal of Geophysical Research-Oceans*, **109**, C06022, doi: 10.1029/2003JC002114.

Appendix 2: Workshops Organized by CRCES

Number	Title	Sponsor(s)	Location	Dates
1.	The NASA-CCR-CRCES Workshop on Decadal Climate Variability	NASA-Physical Oceanography, NOAA-Office of Global Programs, NSF-Climate and Large-scale Dynamics Program	Madison, Wisconsin	15-17 Oct. 2002
2.	The CRCES-IPRC Workshop on Decadal Climate Variability	NASA-Physical Oceanography, NOAA-Office of Global Programs, NSF-Climate and Large-scale Dynamics Program, Univ. of Hawaii	Kona, Hawaii	23-26 Feb. 2004
3.	The CRCES Workshop on Decadal Climate Variability	NASA-Physical Oceanography, NOAA-Office of Global Programs, NSF-Climate and Large-scale Dynamics Program	Warrenton, Virginia	17-20 Oct. 2005
4.	The Workshop on Monsoon Climate Variability and Change, and Their Impacts on Water, Food, and Health in Western India	NSF-Climate and Large-scale Dynamics Program, NASA-Precipitation Science Program, Department of Science and Technology (Govt. of India), Nirma University of Science and Technology (Ahmedabad, India)	Ahmedabad, India	5-7 Feb. 2007
5.	The CRCES Workshop on Societal Impacts of Decadal Climate Variability on the U.S.	NOAA-Sectoral Applications Research Program, U.S. Geological Survey, U.S. Army Corps of Engineers – Institute for Water Resources	Kona, Hawaii	26-28 Apr. 2007
6.	The Seventh Workshop on Decadal Climate Variability	NASA-Physical Oceanography, NOAA-Office of Global Programs, NSF-Climate and Large-scale Dynamics Program	Kona, Hawaii	30 Apr.-3 May 2007
7.	Workshop on Decade-Long Drought and Wet Periods in the Missouri River Basin	NOAA-Sectoral Applications Research Program	Kansas City, Missouri	27-28 Apr. 2009
8.	Workshop on Decade-Long Drought and Wet Periods in the Missouri River Basin	NOAA-Sectoral Applications Research Program	Helena, Montana	24-25 Jun. 2009
9.	The Eighth Workshop on Decadal Climate Variability	NASA-Physical Oceanography, NSF-Climate and Large-scale Dynamics Program, DOE-Office of Biolog. and Environ. Research	St. Michaels, Maryland	12-15 Oct. 2009
10.	Workshop on Decade-Long Drought and Wet Periods in the Missouri River Basin	NOAA-Sectoral Applications Research Program	Lincoln, Nebraska	16-17 Nov. 2010
11.	Workshop on Impacts of Decadal Climate Variability on the Great Falls Urban Water System	NOAA-Sectoral Applications Research Program	Great Falls, Montana	9 Oct. 2012

12.	Workshop on Impacts of Decadal Climate Variability on the Lincoln Urban Water System	NOAA-Sectoral Applications Research Program	Lincoln, Nebraska	11 Oct. 2012
13.	Workshop on Impacts of Decadal Climate Variability on the Kansas City Urban Water Systems	NOAA-Sectoral Applications Research Program	Kansas City, Missouri	12 Oct. 2012
14.	Workshop on Adaptation of Water and Agriculture Sectors to Decadal Climate Variability in the Marias Sub-basin in the Missouri River Basin	NOAA-Sectoral Applications Research Program	Great Falls, Montana	20 Nov. 2013